Tetrahedron 68 (2012) 8945–8967

Contents lists available at SciVerse ScienceDirect

Tetrahedron

journal homepage: www.elsevier.com/locate/tet

Design, synthesis and structure of new dendritic melamines. First use of a tandem C-2-substituted serinol—*O*,*O*-masked 4-piperidone as a peripheral unit in iterative synthesis

Flavia Popa [a,b], Pedro Lameiras [c], Oana Moldovan [a,b], Maria Tomoaia-Cotisel [a], Eric Henon [c], Agathe Martinez [c], Carmen Sacalis [a], Aurora Mocanu [a], Yvan Ramondenc [b], Mircea Darabantu [a,*]

[a] *"Babes-Bolyai" University, Department of Chemistry, 11 Arany Jànos st., 400 028 Cluj-Napoca, Romania*
[b] *University and INSA of Rouen, IRCOF—LCOFH, UMR 6014 CNRS COBRA, 76821 Mont Saint-Aignan Cedex, France*
[c] *University of Reims Champagne-Ardenne, ICMR-LIS, UMR 6229, BP 1039, 51687 Reims, France*

ARTICLE INFO

Article history:
Received 9 October 2011
Received in revised form 27 June 2012
Accepted 31 July 2012
Available online 5 August 2012

Keywords:
Dendrimers
Melamines
Serinols
4-Piperidone
NMR
AFM (atomic force microscopy)

ABSTRACT

The iterative chemoselective amination of cyanuric chloride to dimers of new G-2 dendritic *N*-substituted-2,4,6-triamino-*s*-triazines (*melamines*) having C-2-substituted 2-aminopropane-1,3-diols ('*serinols*') in tandem with the ethylene ketal of 4-piperidone as peripheral units is reported. The structure as a function of increasing molecular size was studied by NMR spectroscopy, DFT calculation and AFM imaging. A concise nomenclature defining the restricted rotational phenomena about the newly created C(*s*-triazine)—N(exocyclic) partial double bonds, seen as axes of (pro)diastereomerism, is used. We propose a new form of frontier rotamerism for the dendrimer surface, which operates over a long range.

1. Introduction

Resulting from pharmaceutical chemistry, *Serinol* is the trivial nomenclature of 2-aminopropane-1,3-diol, seen as the reduced form of *Serine* and the parent term for a series of compounds comprising its commercial C-2-substituted analogues **A**–**C** (Chart 1).[1,†]

It was in 1985 when Newkome et al.[2] used TRIS (**C**) in the synthesis of the first so-called '*arborol*' that the chemistry of dendrimers came about. Subsequent developments of these 'cascade syntheses'[3] suggested that TRIS could be a very attractive serinolic building-block for dendritic structures. It could, for example, play several roles within such structures: peripheral unit, tetravalent branch cell and core.[2b] Both *Serinol* itself, as well as its cyclic acetals, proved of interest in the fields of biomedicine[4a–f] and nanomaterials[4g,h] for dendritic constructions of macromolecules. No attention, however, has been hitherto paid to *Methylserinol* **A** and *Ethylserinol* **B**.

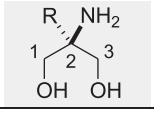

R = H		Trivial name
2-aminopropane-1,3-diol		*Serinol*
C-2-substituted serinols		
Symbol	R	Trivial name
A	Me	*"Methylserinol"*
B	Et	*"Ethylserinol"*
C	CH_2OH	TRIS®, THAM

Chart 1. The C-2-substituted serinols' family.

The last decade has seen much development in the field of melamine-based dendrimers. This has flowed from the first results of Simanek et al.,[5a] in 2000. There have been various approaches to this new class of macromolecule taken. First, in the domain of iterative convergent[5a–f] versus divergent syntheses,[5a,g–m] one such approach consisted in the adding the 'classic' (but still useful) chemoselective amination of cyanuric chloride. Not long after

* Corresponding author. Tel.: +40 264 59 38 33; fax: +40 264 59 08 18; e-mail addresses: darab@chem.ubbcluj.ro, darabantu@cluj.astral.ro (M. Darabantu).

† The C-1-substituted *serinols* are also commercial as chiral (1*S*,2*S*)-'phenylserinols', e.g., R=Ph or *p*-nitrophenyl.

0040-4020/$ – see front matter © 2012 Elsevier Ltd. All rights reserved.
http://dx.doi.org/10.1016/j.tet.2012.07.096

the publication of those results, Simanek et al. managed to effect manipulations specifically relating to the peripheral groups of dendritic melamines.[6] In so doing, they highlighted two major applications, organic nanomaterials[7] and vehicles for drug delivery systems.[8] All this has been described several recent reviews.[9]

The amination of cyanuric chloride with *C*-substituted (masked) serinols, such amination being combined with targeting bioactive *N*-substituted melamines, has, however, scarcely been touched since 1979.[10a,b] Our group has previously reported on the convergent synthesis of the first serinolic G-2 melamine dendrimer incorporating (1*S*,2*S*)-*p*-nitrophenylserinol as peripheral units.[11a,b] We also reported on our failure to arrive at similar structures based on C-2-substituted serinols **A**–**C** (Chart 1).[11b] In the course of our search for an additional challenging amino-nucleophile (in tandem with serinols **A**–**C** in a new iterative synthesis of melamines), we began to consider the ethylene ketal of piperidone. This compound is relevant[12] in nucleophilic substitution of chlorine in certain chlorodiamino-*s*-triazines, such substitution being carried out with 4-piperidone derivatives. This provides pharmaceutical compositions for treating pathological states that arise from, or are exacerbated by, angiogenesis.[12]

So the aim of the present full report is to give an account of the first melamine G-2 dimeric dendrimers (convergent synthesis, structure and dynamic behaviour) that have the tandem C-2-substituted serinol—*O*,*O*-masked 4-piperidone as peripheral units. The compounds, to which the title of this paper refers, combine, then, three 'traditional' biological units (serinols, *s*-triazine and 4-piperidone) but in a dendritic context.

2. Results and discussion

2.1. Synthesis

2.1.1. Preliminary inspection of reactivity of 4-piperidone and its ethylene ketal with cyanuric chloride. As early as 1999,[12] the selective installation of a piperidine type motif as the first amino-nucleophile on cyanuric chloride seemed to be not recommended. Later on, Simanek's convincing 'relative reactivity maps'[5d,f,j] that focused on elaborating dendritic melamine[5i,h] confirmed this negative observation. Furthermore, the instability of 4-piperidone free base with respect to autocondensation has been common knowledge since 1949.[13a] Therefore the use instead of its stable hydrochloride derivatives, 'monohydrate' **1** or ethylene ketal **2** is suitable (Scheme 1). In the context of these premises, we have previously reported[11b,13b–d] satisfactory results in the syntheses shown in Scheme 1. Both salts, **1** and **2** (the latter freshly prepared, according to Bickelhaupt et al.[13e]), exhibited a notably reduced solubility in the anhydrous solvents that are usually used for this chemistry (THF, 1,4-dioxane, chloroform and dichloromethane). Combined with the insolubility of our inexpensive proton scavenger (K_2CO_3) in the same solvents, the corresponding free bases were not quickly generated from **1** and **2**. By contrast, a rapid acid–base interchange between **1** or **2** and K_2CO_3 occurred in 10% aq THF, and the in situ resulting amino-nucleophiles showed high strength. Indeed, the displayed results in the syntheses **1**→**1a** and **2**→**2a** were due to manipulations in very mild conditions only. These conditions ensured complete chemoselectivity for di- versus trisubstitution of chlorine in cyanuric chloride.

These preliminary data suggested to us our next steps:

(i) Careful monitoring of 4-piperidone based nucleophilic species when selective S_N2Ar aminations are envisaged.

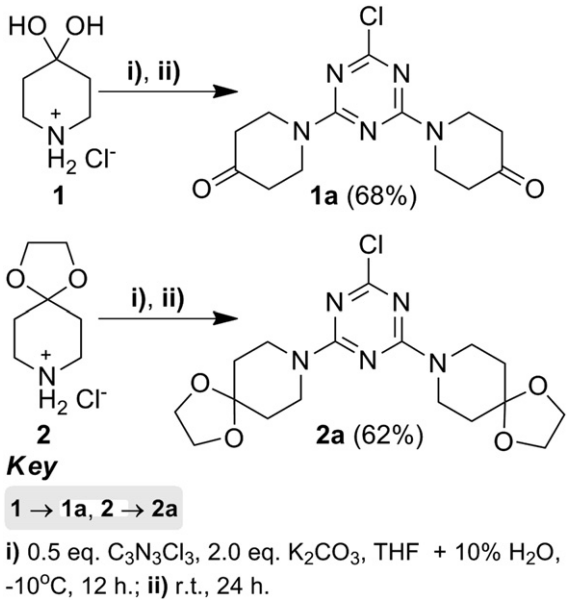

Scheme 1.

(ii) The opportunity to consider the new chlorodiamino-*s*-triazines **1a** and **2a** as simpler structures, i.e., 'model compounds', for subsequent dendritic architectures that would incorporate these motifs. We have previously discussed the relevance of this 'structural simulation',[11b] around the same time as Simanek et al.[14]

2.2. Synthesis of G-0 melamines. Selective installation of peripheral units and of the first linker

Our first object of enquiry was the series of new melamines **6a**–**e** (Scheme 2, steps **I**–**III**; Table 1).

Initially, we followed three related lines of enquiry, series **a**–**c**, starting from serinols **A**–**C** in tandem with the ethylene ketal of piperidone **2** (Scheme 1). Next, the optimised results (Table 1, entry 3 vs 2) encouraged us to consider two additional directions, **d** and **e**, by including in our study the less polar 2-amino-2-methylpropanol (**D**).[15a] Just as had been the case with **A**–**C**, the role for **D** was as a peripheral unit, whether in combination with **2** (series **d**), or alone (series **e**). The opening step (amination **I**), performed with the weaker amino-nucleophiles **A**–**D**, was routine (Table 1, entry 1), with TLC monitoring indicating completion in all cases **3a**–**d**. By contrast, in amination step **II**, the selective preparation of unsymmetrically *N*,*N*′-substituted chlorodiamino-*s*-triazines **4a**–**d** (Table 1, entry 2 vs 3) required (i) low temperature and (ii) slow gradual addition of **2** to the reaction mixtures that contained the non-isolated **3a**–**d**. Under these conditions, TLC control confirmed, besides total consumption of these intermediates (Table 1, entry 3), minimum incidence of side reactions, e.g., complete amination (→melamines **5a**, **5b**, Table 1, entry 2) and possible contaminating hydroxylation and/or alkoxylation of **3a**–**d**.[16]

The one-pot synthesis (steps **I**+**II**) of symmetrically *N*,*N*′-substituted chlorodiamino-*s*-triazine **4e** (Table 1, entry 4) was simple and clean, with good yield.

In step **III**, we effected, in accordance with our previously published method, the selective anchorage of the first piperazine linker (Table 1, entry 5).[11,13c] We detected symmetric double melamines **7** as side products and isolated them using column chromatography on partially deactivated silica gel (*i*-PrOH or EtOH/aq 25% NH_3 9:1) in only three cases, **7a**, **7b** and **7e**. Our explanation for the observed chemoselectivity makes use of an alternative synthesis (Scheme 2) of dimeric G-0 melamines **7a**

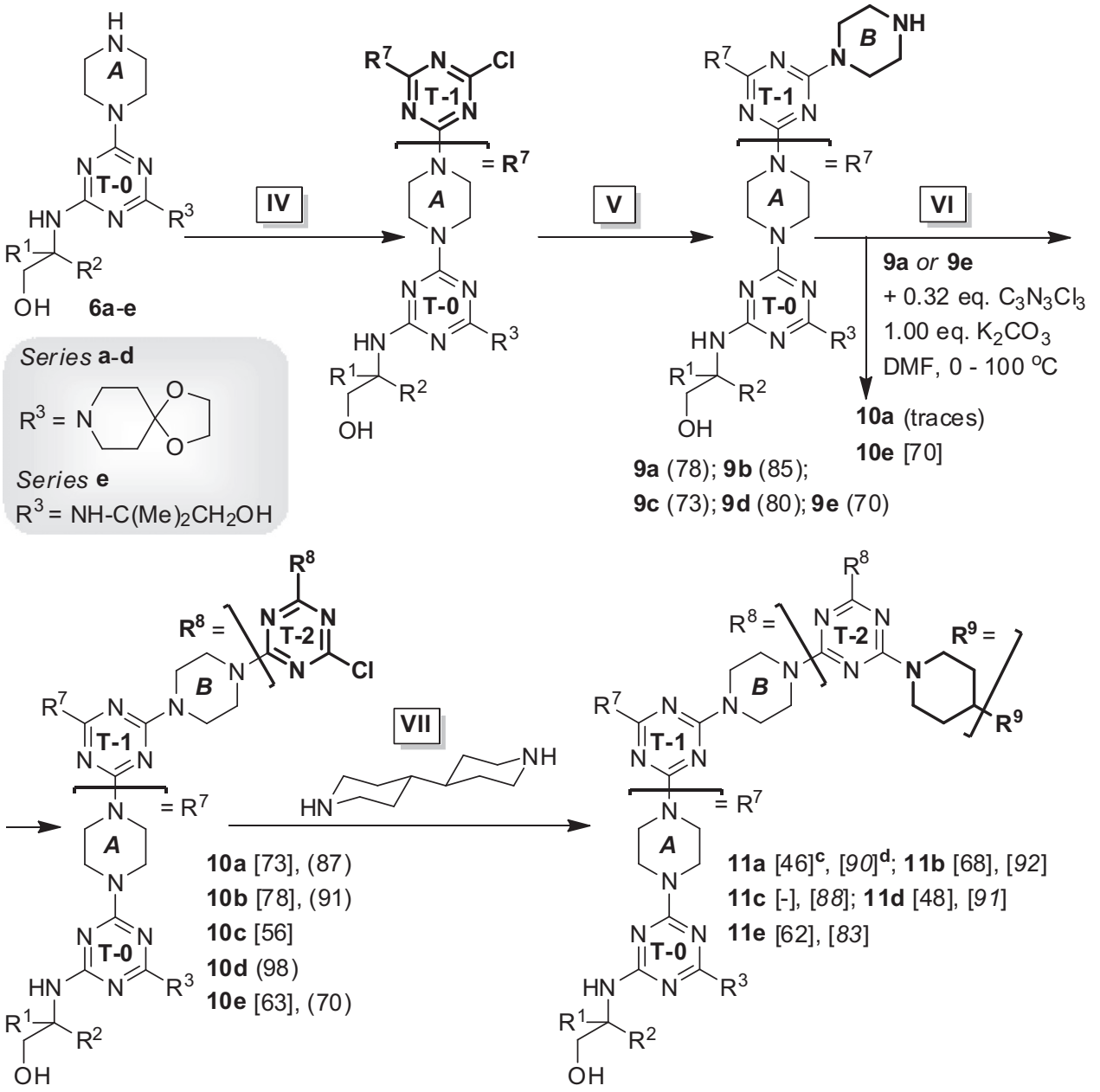

[a]In square brackets: yield after isolation by column chromatography; [b]In round brackets: yield after isolation by direct crystallisation; [c]In series **11**: yields by neglecting the recovered as unreacted **10**; [d]Conversions of **10**.

***Key* IV**: **i)** 0.45 eq. $C_3N_3Cl_3$, 1.00 eq. K_2CO_3, THF, (-10°C) → r.t., 12 h.; **ii)** 1,4-dioxane, reflux: 11 h. (**8a**), 12 h. (**8b**), 16 h. (**8c**), 8 h. (**8d**), 11 h. (**8e**).

V: 4.00 eq. piperazine, 1.00 eq. K_2CO_3, 6 × 0.16 eq. **8a-e**, THF, reflux, 6 × 1.5 h.

VI: **i)** 0.48 eq. $C_3N_3Cl_3$, 1.00 eq. K_2CO_3, THF. (-10°C) → r.t., 12 h., reflux, 16 h.; **ii)** 1,4-dioxane, reflux, 6 h.

VII: 0.48 eq. 4,4'-bipiperidine, 1.00 eq. K_2CO_3, DMF, 100°C, 36-72 h.

Scheme 2.

and **7e**. The reaction between piperazine and 2.03 mol equiv of **4a** or **4e** in the presence of K_2CO_3, needed 12 h in refluxing 1,4-dioxane to yield **7a** (87% yield) and **7e** (76% yield). To explain these results, we suggest that the transannular effect of piperazine favours its mono-*N*-substitution. This effect was previously noticed by Lai et al.[7e,f]

2.3. Synthesis of G-1, -2 dendritic melamines. Feasibilities and failures

Our next study involved the twofold anchorage of melamines G-0 **6a**–**e** (step **IV**, Scheme 3) to cyanuric chloride. From this we produced G-1 chlorodendrons **8a**–**e**. As in step **II**, where the

Table 1
Results and conditions in the synthesis of compounds **4**–**7**

Step	Entry	Molar ratios	Reaction conditions	Main and by-products (yields, %)
I	1	1.00 **A**–**D** 1.00 $C_3N_3Cl_3$ 1.00 K_2CO_3	THF, rt, 24 h	**3a**–**d** not isolated
II	2	1.00 (**2**) 2.00 K_2CO_3	THF+10% H_2O (i) (−12 °C), 12 h (ii) →rt, 12 h (iii) rt, 24 h	**4a** [53][a]+**5a** [4] **4b** [58]+**5b** [5] **4c** (76)
	3	5×0.20 (**2**)[b] 2.00 K_2CO_3	THF+10% H_2O (i) (−12 °C), 5×1.5 h[b] (ii) 36 h., (−15 °C)	**4a** (83) **4b** (87) **4d** (85)
I+**II**	4	0.49$C_3N_3Cl_3$ 1.00 K_2CO_3	THF (i) (−10 °C→rt), 12 h (ii) rt, 12 h (iii) 45 °C, 13 h	**4e** (75)[c]
III	5	4.00 piperazine 1.00 K_2CO_3 6×0.16 (**4a**–**e**)	THF, rt, 6×1.5 h	**6a** [89]+**7a** [6] **6b** [87]+**7b** [1] **6c** (78) **6d** (82) **6e** [85]+**7e** [5]

[a] In square brackets: for compounds **4a** and **4b** as partial conversions of cyanuric chloride into the depicted compounds; for compounds **6a**, **6b** and **6e** as partial conversions of their corresponding precursors, **4a**, **4b** and **4e**.
[b] Five equal portions of **2** (Scheme 1) each 1.5 h.
[c] Our result; according to literature,[15a] no yield was reported for this compound but a general procedure published previously, in the period of 1950.[15b]

peripheral hydroxyl groups were unprotected, we began our manipulations at low temperature in THF, continued them at room temperature and finished in refluxing 1,4-dioxane. The more taxing conditions required for this step **IV** were justified on account of the high solvation in THF and 1,4-dioxane of our nucleophiles **6a**–**e**. For a satisfactory or good yield from this double amination, the process required a 10% molar equivalent excess of **6a**–**e**/1 equiv chlorine in cyanuric chloride.

It was, furthermore, equally necessary to adopt the more taxing conditions of refluxing THF for step **V**, which involved the mono-attachment of the second piperazine linker *B* to chlorodendons **8a**–**e**. We followed an experimental protocol that was the same as that adopted for step **III** (Scheme 2). No side-product dimeric G-1 melamines, analogues of G-0 **7**, were detected. Yields, however, of melamines G-1 **9a**–**e** when compared to those of melamines G-0 **6a**–**e**, were slightly smaller. Our tentative explanation relates to the higher relative retention on column chromatography.

Surprisingly, although the final installation of a trivalent *s*-triazine core is commonly used in the synthesis of dendritic melamines,[5f–k,7b,h,8b,c,e,f,14] the attempted triple amination of cyanuric chloride with G-1 dendrons **9a** and **9e** was unsuccessful, presumably because of the 'starburst effect'.[17] Starting from **9a**, decomposition of the organic material occurred as both NMR and TLC of the crude reaction mixture evidenced. In the mass spectrum (MALDI+), we found that the molecular peak was only consistent with formation of the G-2 chlorodendron **10a**. Our treatment of cyanuric chloride with 3.15 mol equiv of **9e** was also disappointing (Scheme 3), only producing chlorodendron G-2 **10e**.

From these failures, we took the view that it was best to avoid similar experimental manipulations that would start from chlorodendrons **9b**–**d**. So we planned a series of experiments having their origin in G-2 chlorodendrons **10a**–**e**, rather than looking for a larger trivalent core. Applying a similar experimental procedure for our next step (**VI**) to the one we applied in step **IV** (Scheme 2), happily resulted in clean reactions and ready work-up.

In the final step, (**VII**), we decided to couple two identical building-blocks **10a**–**e** via a secondary diamine central linker. Piperazine is repeatedly mentioned in the literature to play such a role.[5a–e,6a–c,7a,7e–h] We were suspicious of the efficacy of this because, given the failures mentioned above, we believed our central linker should be larger. Therefore, since Simanek et al.[5k] recently reported the use of 1,3-di(piperidin-4-yl)propane ('*trimethylenedipiperidine*') in a protective–deprotective strategy, we considered the use of 4,4′-bipiperidine. This diamine (commercially available as dihydrochloride) has not hitherto been the object of enquiry with respect to dendritic melamine chemistry.

Initial experiments revealed that (i) DMF was the most suitable solvent in circumstances where the temperature did not exceed 100 °C, (ii) the 4,4′-bipiperidine free base should be generated first in a separate experiment[18] and (iii) a 2:1.1 molar ratio of **10a**–**e**/4,4′-bipiperidine worked best. MS spectra of the crude reaction mixtures displayed, in accord with TLC, the same two types of component in each case: the unreacted **10a**–**e** and desired **11a**–**e**. No molecular peak consistent with the presence of a mono-*N*-substituted-4,4′-bipieridine was detected.

Direct crystallisation as a separation technique was only feasible in the case of mixture **10b**+**11b** when the yield (69%) was almost the same as the yield achieved by column chromatography on silica gel (68%). As the results demonstrated, in spite of some promising conversions of dendrons **10a**–**e**, yields were affected, overall, by retention of **11a**–**e** on silica gel. Except in the case of **11c**, all dendrimers provided credible analytical data (see Supplementary data 'SD' and Experimental section). The seven-step **I**–**VII** convergent synthesis of G-2 dendritic melamines **11a**, **11d** and **11e** produced consistent global yields of 17–18%. However, starting from *Ethyl-serinol* (**B**), the best result in the case of dendrimer **11b** was 31%. The explanation for this remains obscure.

Two additional negative results should also be mentioned:

(i) The failure to isolate compound **11c** as a pure analytical sample.

The unreacted **10c** was recovered easily by using $CHCl_3$/MeOH/Et_2O 3.5:1.0:0.5 but eluting with $CHCl_3$/MeOH 3.5:1.0 to give **11c**, promoted its partial decomposition. Despite its credible MS analysis (see later on, Fig. VIc in SD 8), in the NMR spectra, including the 2D ^{1}H DOSY experiment, **11c** was the single macromolecular species (Fig. VIId in SD 9), i.e., a component of a mixture of compounds with lower molecular size.

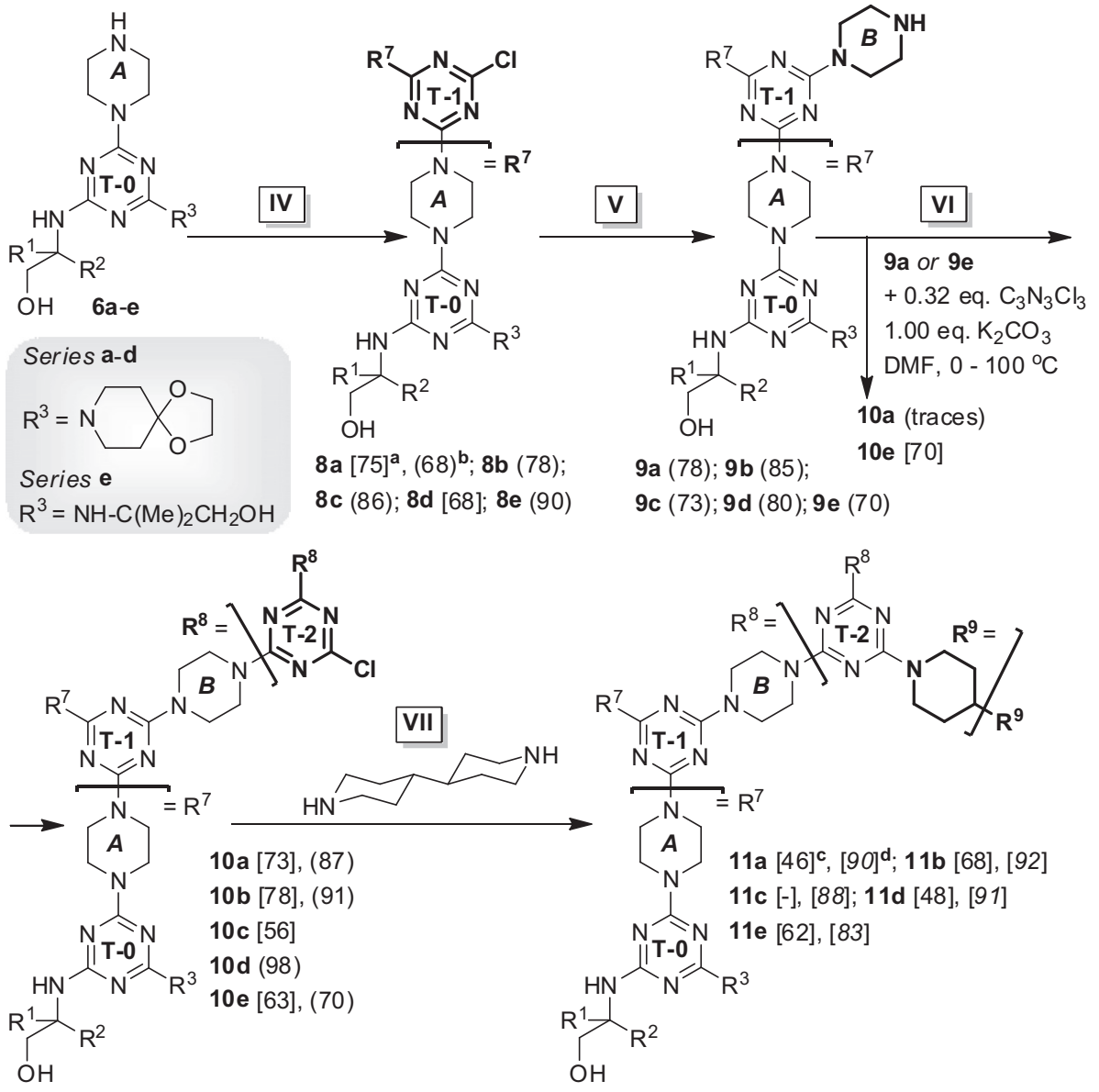

[a]In square brackets: yield after isolation by column chromatography; [b]In round brackets: yield after isolation by direct crystallisation; [c]In series **11**: yields by neglecting the recovered as unreacted **10**; [d]Conversions of **10**.

***Key* IV**: **i)** 0.45 eq. $C_3N_3Cl_3$, 1.00 eq. K_2CO_3, THF, (-10°C) → r.t., 12 h.; **ii)** 1,4-dioxane, reflux: 11 h. (**8a**), 12 h. (**8b**), 16 h. (**8c**), 8 h. (**8d**), 11 h. (**8e**).

V: 4.00 eq. piperazine, 1.00 eq. K_2CO_3, 6 × 0.16 eq. **8a-e**, THF, reflux, 6 × 1.5 h.

VI: **i)** 0.48 eq. $C_3N_3Cl_3$, 1.00 eq. K_2CO_3, THF. (-10°C) → r.t., 12 h., reflux, 16 h.; **ii)** 1,4-dioxane, reflux, 6 h.

VII: 0.48 eq. 4,4'-bipiperidine, 1.00 eq. K_2CO_3, DMF, 100°C, 36-72 h.

Scheme 3.

(ii) The failure to deprotect the *O*,*O*-masked 4-piperidone peripheral units.

Final *N*-, *O*- or *S*-deprotection of peripheral groups in dendritic melamines is one of the strategies of choice in their synthesis.[5] In our case, however, all our attempts to apply to dendrimers **11a**, **11b** and **11d** the deprotecting protocol that had previously been reported by us in the case of compound **2a** (Scheme 1)[13b,d] failed. This was the case even under much milder conditions. The dendrimers rapidly decomposed.

3. Structural investigations

3.1. Analysis in solution by NMR techniques. Dynamic phenomena versus solvation effects

As early as 1971,[19a] it was established that the C^{sp2}(*s*-triazine)–N^{sp3} connections have a partial double bond character[19,20] due to the p → π conjugation between the lone pair of the exocyclic N-atom in conjunction with the high π-deficiency of the *s*-triazine ring. There is a restricted rotation thereby induced. Variable tem-

Two axes of prodiastereomerism

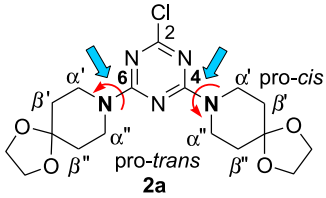

Expected rotational status about bonds C(*s*-triazine)-N(exocyclic)

Frozen ➔ C(4, 6)-N(exocyclic): axes of *prodiastereomerism*

Freely rotating ↻ *Homomeric* rotation (*topomerisation*) equilibrating equally populated sites

Found (VT) ^{1}H NMR data as δ (ppm), appearance,[a] in [D$_6$]DMSO on 500 MHz timescale

➔ *Frozen* (293 K)

1st "*internal clock*"[22a]		2nd "*internal clock*"[22a]	
H-α'	H-α"	H-β'	H-β"
3.78 (bt)	3.74 (bt)	1.63 (bt)	1.62 (bt)

Slowly rotating (coalescences, T_c K)

3.77 (308)	1.63 (298)

↻ *Freely rotating (Fast exchange)* (343 K)

3.78 (t)	1.65 (t)

Pseudo freely rotating (353 K)

3.79 (ot), 3.78 (ot)	1.66 (t)

Found $\Delta G^{\neq}$ (kJ/mol) as barriers to rotation at T_c

65.86 (308)[b]	66.36 (298)[b]

66.11±0.25

[a]Specific abbreviations: (bt) broad triplet; (ot) overlapped triplet; [b]Eyring algorithm was used (SD 1).[22b, 22c]

Chart 2. Rotational prodiastereomerism of 'model compound' **2a** as issued from (VT) ^{1}H NMR data.

perature NMR spectroscopy is an appropriate technique for monitoring this.[20]

The effect of this phenomenon on iterative amino-*s*-triazine synthesis, however, has been much less well-studied.[11,14,21] We therefore resolved to examine, from rotational point of view, the status (static or dynamic) of our five series of compounds **a**–**e**. We revisited the terminology that we had recently proposed.[11b,13d,21] This applies where C(*s*-triazine)–N(exocyclic) partial double bonds are seen as innate *(pro)stereogenic axes, i.e., axes of prodiastereomerism* or *axes of diastereomerism*. On rising the temperature, the free motion acquired is described as *homomeric* (*topomerisation*) or *diastereomeric*.

3.1.1. G-0 chlorodendrons. Solvation determining rotameric abundance. Our analysis started with a brief (VT) ^{1}H NMR inspection of the a priori designed 'model compound', the *N,N′*-symmetrically substituted chlorodiamino-*s*-triazine **2a** (Scheme 1, Chart 2, SD 1).[13d]

At room temperature, the discrimination between azaspiranic diastereotopic positions as $\delta_H(\alpha')>\delta_H(\alpha'')$ and $\delta_H(\beta')>\delta_H(\beta'')$ was made based on the closer proximity of nuclei α′ and β′ against α″ and β″ with respect to the dipole moment of bond C-2(*s*-triazine)–Cl, i.e., this bond was considered a strong deshielding factor.[8d,11b,21] For the present discussion, we will henceforth call this assignment 'the dipole rule'.[11b,13d,21] Compound **2a** reached *freely rotating status* (*fast exchange*) at 343 K.[22a–c] To our surprise, when temperature was increased further, at 353 K, a new anisochrony was exhibited by methylenes H-α. As this chemical non-equivalence was only 14.5 Hz, the hypothesis that it could originate from a geminal diastereotopicity induced by the well-documented axial chirality in spiranes could be ruled out.[23] We therefore called this unexpected dynamic behaviour of compound **2a** its *pseudo freely rotating* status. This could be caused by some residual steric hindrance between the two azaspiranic fragments preventing complete fast rotation, combined with the pyramidal inversion of their aza-atoms.[20e,f]

Next, we turned our attention to the unsymmetrically *N,N′*-substituted chlorodiamino-*s*-triazines **4a**–**d** (Tables 2 and 3). Once again the rotational analysis appears to be original to us.[13d,21b] Only symmetrically *N,N′*-substituted chlorodiamino-*s*-triazines have been investigated in this way before.[11b,20b,c]

At 293 K, a two-term frozen diastereomerism occurred about the bond C-6(*s*-triazine)–N(exocyclic) and was non-statistical. Two blocked rotamers **4a**–**d**-*anti* (major) and **4a**–**d**-*syn* (minor) were preliminarily assigned according to the 'dipole rule' applied, this time, to protons NH and OH (Table 2, Fig. I in SD 2). However, the 2D-^{1}H, ^{1}H-NOESY charts were unable to disclose any dipolar interaction between amino(poly)olic and azaspiranic sites in any of the rotamers of series **4a**–**d** a priori designed as *anti*. Therefore, a DFT calculation in the case of compound **4a** was performed, despite the fact that the ratio between the two rotational states of **4a**–**d** (around 75:25 *anti*/*syn*) was consistent with a $\Delta\Delta G_{298} \sim -2.72$ kJ/mol, i.e., less than 1 kcal/mol. The results are summarised in Table 3.

For each rotamer **4a**-*anti* and **4a**-*syn*, three conformers about serinolic the NH–C^{sp3} bond were optimised. Only the B3LYP/6-311++G**/CPCM/model provided results in line with our postulated 'dipole rule'. In DMSO, plausible barriers to rotation $\Delta G^{\neq}$ (*syn*⇄*anti*) were found if compared to those resulting from the VT ^{1}H NMR spectral analyses (see Table 2 and later discussion).[‡]

At room temperature, the rotational prodiastereomerism was detectable on the ^{13}C NMR timescale only as diastereotopicity $\Delta\delta_C$ between azaspiranic positions α′ versus α″ and β′ versus β″ in the major *anti* rotamer (Table 2). On ^{1}H NMR spectra, the signal resolution of protons H-α and H-β was not amenable for kinetic calculations (Table 2; Fig. I in SD 2; Fig. II in SD 3). Upon heating, no clear coalescence was observed for H-α. For H-β, a $T_c \sim 308$ K, found earlier for H-α in the 'model' compound **2a** (Chart 2), was assigned in series **4a**–**d**. As in the case of **2a**, the final dynamic status of compounds **4b**–**d** was a global *pseudo freely rotating* one. We felt we had to conclude that the *local homomeric rotation* (*topomerisation*) about the C(4)–N(exocyclic) bonds in unsymmetrical compounds **4a**–**d**, was similar to that of symmetric *s*-triazine **2a**, hence $\Delta G^{\neq}=66.11\pm0.25$ kJ/mol.

The analysis in serinolic sequence about the C(6)–N(exocyclic) bonds focused on a process equilibrating two unequally populated sites, **4a**–**d**-*anti*>**4a**–**d**-*syn*. Accordingly, two $\Delta G^{\neq}$ values, $\Delta G^{\neq}_{anti}(a\rightarrow s) > \Delta G^{\neq}_{anti}(s\rightarrow a)$, defining two first-order kinetic processes, were evaluated by applying the method of Shanan-Atidi[22d] (Table 2; Table I in SD 4).

The same type of calculation was then carried out for symmetrically *N,N′*-substituted chlorodiamino-*s*-triazine **4e** in which, at room temperature, the C(*s*-triazine)–N(exocyclic) partial double bonds were two axes of diastereomerism. Consequently, we had to take into account an equilibrium involving three components (Chart 3).

According to the 'dipole rule', a distinction between frozen rotamers, **4e**-(*a*–*a*), -(*a*–*s*) and -(*s*–*s*) was made. In order to

[‡] More rigorously, if *all three conformers* in each series **4a**-*anti* and **4a**-*syn* are considered together with the Boltzmann statistics of their energy level population, the calculated rotameric ratio was *anti*/*syn* 64:36.

Table 2
Two terms rotational (pro)diastereomerism of compounds **4a**–**d** as issued from (VT) NMR data

One axis of prodiastereomerism and one axis of diastereomerism

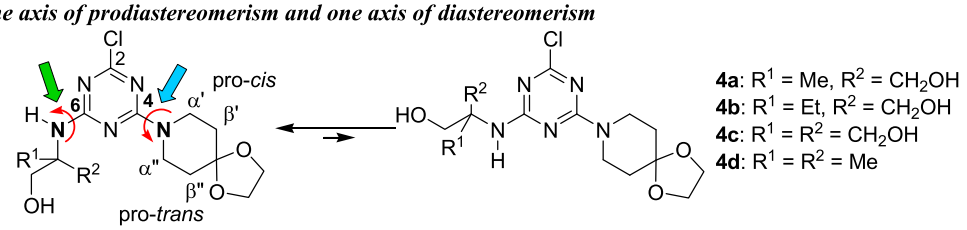

*anti** (*a*) → **4a-d**-*anti* *syn* (*s*) → **4a-d**-*syn*

*The chlorine atom and the *C*-substituted (poly)olic fragment are the references for the descriptors *anti* and *syn*.

Expected rotational status about bonds C(*s*-triazine)-N(exocyclic)								
Frozen	→ C(4)-N(exocyclic): axis of prodiastereomerism							
	→ C(6)-N(exocyclic): axis of diastereomerism							
Local freely rotating	↻ *Homomeric* rotation (*topomerisation*) about the bond C(4)-N(exocyclic)							
	↻ *Diastereomeric* rotation about the bond C(6)-N(exocyclic)							
Global freely rotating	↻ *Diastereomeric* rotation equilibrating two unequally populated sites							
Found (VT) NMR data as δ (ppm), appearance, in [D₆]DMSO								
→ → *Frozen* (293 K)								
δ (ppm)	**4a** (%)			**4b** (%)		**4c** (%)		**4d** (%)
	anti ⇆ *syn*			*anti* ⇆ *syn*		*anti* ⇆ *syn*		*anti* ⇆ *syn*
	75.4[a]		24.6[a]	77.9	22.1	72.8	27.2	79.4	20.6
NH	6.94 (s)		6.75 (s)	6.83 (s)	6.65 (s)	6.67 (s)	6.54 (s)	7.25 (s)	7.03 (s)
OH	4.63 (t)		4.74 (t)	4.56 (t)	4.68 (t)	4.52 (bs)		4.74 (t)	4.84 (t)
H-α	3.74 (bs)			3.72 (t)		3.73 (t)		3.78-3.72 (bm)	
H-β	1.66-1.59 (bm)[b]			1.65-1.59 (bm)		1.67-1.60 (bm)		1.66-1.59 (m)	
C-α', -α"	42.0 41.8		41.4	42.1 41.9	41.4	42.1 41.9	41.5	42.0 41.8	41.4
C-β', -β"	34.8 34.5		-[c]	34.9 34.6	34.8	35.0 34.8	34.9	34.8 34.6	-[c]
Slowly rotating (coalescences, T_c K)									
NH	6.61 (338)			6.50 (338)		6.46 (328)		6.84 (338)	
OH	4.53 (338)			4.43 (338)		-		4.63 (328)	
H-α	-			-		-		3.75 (298)	
H-β	1.63 (308)			1.63 (308)		1.63 (308)		1.62 (308)	
↻ *Global freely rotating* (353 K) **4a**				*Global pseudo freely rotating* (353 K) **4b-d**					
NH	6.53 (bs)			6.41 (bs)		6.35 (bs)		6.75 (bs)	
OH	4.46 (bs)			4.40 (bs)		4.33 (bs)		4.56 (bs)	
H-α	3.80 (t)[d]			3.77 (ot) 3.76 (ot)		3.77 (ot) 3.76 (ot)		3.78 (ot) 3.77 (ot)	
H-β	1.66 (t)[d]			1.66 (ot) 1.65 (ot)		1.66 (t)		1.66 (t)	
Found $\Delta G^{\neq}$ (kJ/mol) as barrier to *homomeric* rotation at T_c									
				66.11 ± 0.25					
Found $\Delta G^{\neq}$ (kJ/mol) as barriers to *diastereomeric* rotation at T_c									
$\Delta G^{\neq}_{anti}(a \rightarrow s)$	71.52 (pred. 69.52)[e]			72.61		70.67		72.28	
$\Delta G^{\neq}_{syn}(s \rightarrow a)$	68.37 (pred. 68.60)			69.07		67.98		68.49	
Found $(\Delta\delta_{NH}/\Delta T) \times 10^3$ (ppb/K) as TG (Temperature Gradient)[f]									
TG	**4a**-(*a*)	**4a**-(*s*)		**4b**-(*a*)	**4b**-(*s*)	**4c**-(*a*)	**4c**-(*s*)	**4d**-(*a*)	**4d**-(*s*)
	-6.83	-3.67		-6.90	-3.90	-5.33	-3.17	-8.33	-4.67

[a]Averaged contents issued from the best separated signals, NH (s) and OH (dd as t) except compound **4c**. [b]Specific abbreviations: (bm) broad multiplet, (ot) overlapped triplet. [c]Overlapped signals. [d](t) at 353 K as typical triplets with $^3J_{H,H}$ = 5.5-6.5 Hz. [e]In round brackets: predicted $\Delta G^{\neq}$ values by calculation at B3LYP/6-311++G** level of theory (see Table 3). [f]$\Delta\delta_{NH} = [\delta_{NH}(T\ K) - \delta_{NH}(T_{r.t.})] < 0$; $\Delta T = (T - T_{r.t.}) > 0$ (K) where T = 353 K and $T_{r.t.}$ is the room temperature, 293 K.[14] See later discussion.

examine, however, their rotational deblocking, we simplified the problem. We have done so in two respects: (i) by neglecting the incidence of the minor rotamer **4e**-(*s*–*s*) and (ii) by considering a single rotation around C(*s*-triazine)–N(exocyclic) bonds/equilibrium. We assume here value of these simplifications on the bases of our previous account of them.[11b,21b,24]

Then, by monitoring the ^{1}H NMR NH line shape against the progressively increasing temperature (Chart 3; Fig. III in SD 5), we deduced that:

(i) A global topomerisation of rotamer **4e**-(*a*–*s*)⇄**4e**-(*s*–*a*), equilibrating two equally populated sites, took place first, most probably via the neglected minor **4e**-(*s*–*s*) (T_c 321 K).

(ii) Deblocking of the most stable **4e**-(*a*–*a*) species occurred at a higher temperature (T_c 336 K), but close to that we already encountered for the unsymmetrical analogues **4a**, **4b** and **4d** (338 K, Table 2). The usage of the Shanan-Atidi algorithm provided kinetic parameters for the equilibrium, 69% **4e**-(*a*–*a*)⇄ 31% **4e**-(*a*–*s*), with **4e**-(*s*–*s*) being approximated as 0%.

Table 3
Bond orders (B.O.), dipole moments μ (D), ZPE corrected relative energies ΔH_{0K} (kJ/mol), relative free energies ΔG_{298} (kJ/mol) and transition states $\Delta G^{\neq}_{298}$ (TS) (kJ/mol) of blocked rotamers of compound **4a** versus their ^{1}H NMR abundance (%)

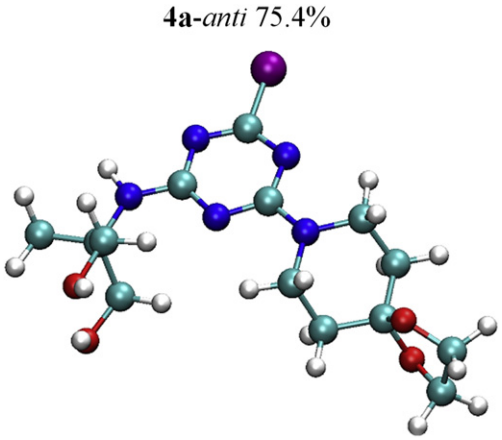

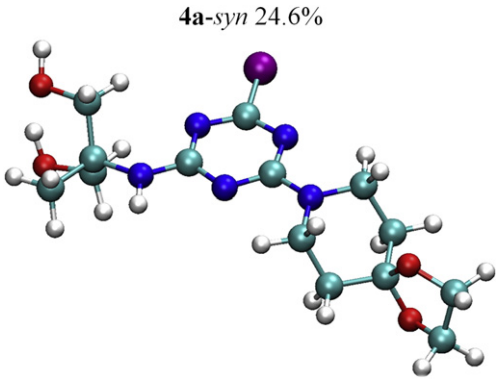

B.O.[a]		μ	ΔH_{0K}	ΔG_{298}	$\Delta G^{\neq}_{298}$ ($a\rightarrow s$)	B.O.		μ	ΔH_{0K}	ΔG_{298}	$\Delta G^{\neq}_{298}$ ($s\rightarrow a$)
C(4)–N<	C(6)–N<					C(4)–N<	C(6)–N<				
B3LYP/6-31G* (gas phase)											
—	—	5.58	2.34	2.34	74.46	—	—	5.31	0.00	0.13	76.72
B3LYP/6-31G*/CPCM/DMSO[b]											
—	—	7.20	0.08	1.05	71.49	—	—	7.17	0.00	0.00	72.53
B3LYP/6-311++G**/CPCM/DMSO											
1.25	1.23	7.30	0.00	0.00	69.52[c]	1.24	1.23	7.86	1.13	0.92	68.60[c]
B3LYP/6-311++G**/CPCM/THF											
—	—	7.03	0.00	0.00	—	—	—	7.50	0.75	0.71	—

[a] Wiberg bond order calculated within the NBO (natural bonding orbital) analysis applied to the depicted C(*s*-triazine)–N(exocyclic) bonds.
[b] The effect of solvent took into account by using the implicit solvent method CPCM (conductor-like polarizable continuum model) implemented in Gaussian 09.
[c] Values to be compared with those provided by VT ^{1}H NMR (Table 2).

Two axes of diastereomerism

Expected rotational status about bonds C(*s*-triazine)-N(exocyclic)

Frozen ➔ C(4, 6)-N(exocyclic): axes diastereomerism

Freely rotating ↻ *Diastereomeric* rotation equilibrating three unequally populated sites

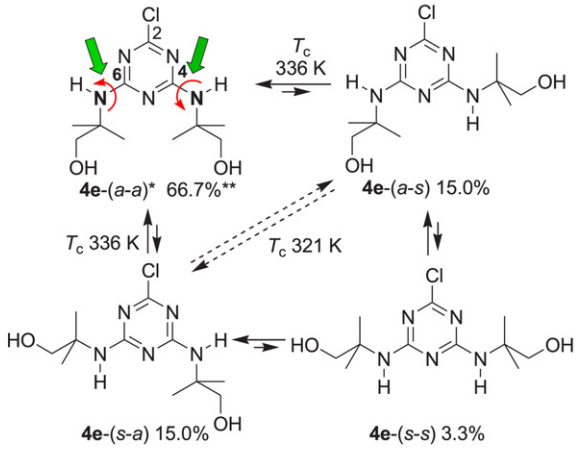

*The chlorine atom and the C-2-substituted propanol fragment are the references for descriptors *anti* (*a*) and *syn* (*s*).
**Percentages uncorrected for symmetry; corrected ratios: 66.7(*a-a*) : 15.0 (*a-s*) : 3.3 (*s-s*); corrected percentages: 78.5% (*a-a*),17.6% (*a-s*), 3.9% (*s-s*).

Found (VT) ^{1}H NMR data as δ_{NH} (ppm) in [D$_6$]DMSO on 500 MHz timescale

➔ *Frozen* (298 K)

(*a-a*)*	(*a*-*s*)	(*s*-*a*)	(*s-s*)
7.07	6.95	6.88	6.55

Slowly rotating (*topomerisation*, T_c = 312 K)

6.92 6.74

Slowly rotating (T_c = 336 K)

6.80

↻ *Freely rotating* (*Fast exchange*) (353 K)

6.65

Found k_c (s^{-1}) and $\Delta G^{\neq}$ (kJ/mol) at T_c

Equilibrium	k_c	$\Delta G^{\neq}$	Method
(*a-s*)⇆(*s-a*)	79.9	65.27	Eyring
(*a*-*s*)→(*a*-*a*)	196.4	67.88	Shanan-Atidi
(*a*-*a*)→(*a*-*s*)	88.3	70.10	Shanan-Atidi

Found $(\Delta\delta_{NH}/\Delta T) \times 10^3$ (ppb/K) as TG

(*a-a*)	(*a*-*s*)	(*s*-*a*)
-7.62	-5.38	-4.07

Chart 3. Three terms rotational diastereomerism of compound **4e** as issued from (VT) ^{1}H NMR data.

All the results reported in this section must, however, be viewed in the light of the following comments. The *s*-triazines **4a**–**e**, seen as G-0 chlorodendrons, were not only the most π-deficient, but also contained the most acidic OH and 'amide like' NH groups. We consider this fact to have possibly important consequences and to place certain 'bounds' on the interpretation of our data.

(i) We had to use ^{1}H NMR parameters of exchangeable NH protons.[22a] This was because they displayed, in all cases, the best separated signals. Nevertheless, according to the δ_{NH} temperature gradients (TG)[14,25] (Table 2), the NH protons were, at room temperature, not exchangeable at all but located in a hydrogen bonding environment provided by the solvent, DMSO-d_6 (vide infra).[20d]

(ii) Barriers to rotation ($\Delta G^{\neq}$) correlated well with the rotameric contents and $\Delta\delta_{NH}/\Delta T$ (temperature gradients, TGs, Table 2 and Chart 3). As recently recommended by Simanek,[14] although this parameter is usually applied to peptides and proteins,[25] it is generally accepted that if the temperature gradient is more negative than −4 ppb/K, in aqueous solution, the NH group is exposed to solvent and not involved in intramolecular hydrogen bonds. In contrast, a temperature gradient less negative than −4 ppb/K indicates that the NH protons are, at room temperature, undergoing intramolecular hydrogen bonding. If so, although the rotameric contents in series **4a**–**d** were comparable, compound **4c**, the most 'hydroxylated', had the smallest $\Delta n = n_{anti} - n_{syn}$ difference, the smallest $\Delta G^{\neq}$ barriers and the least negative TGs. Compound **4c** was the least able to provide its NH groups to the solvent for hydrogen bonding. The internal hydrogen bonding ability of the three geminal hydroxymethyl units of **4c** is responsible for this. Consequently, the ground state of compound **4c** was the least stabilised by solvent. By contrast, for the most NH···DMSO solvated G-0 chlorodendron, the 'mono-hydroxylated' **4d**, we found the highest Δn, TG and $\Delta G^{\neq}$ values.

(iii) The dominant incidence of rotamers **4a**–**d**-(*a*) and **4e**-(*a*–*a*), where these have TG <−4 ppb/K, can also be explained by stronger NH hydrogen bonding with DMSO, in comparison with the *syn* analogues where TG >−4 ppb/K. The *syn* compounds appeared to form internal hydrogen bonds. Overall, 'mono-hydroxylated' compounds **4d** and **4e** were, regardless their rotamerism, the most NH solvated, as their TGs disclosed.

(iv) The increasing sequence of $\Delta G^{\neq}$ values $\Delta G^{\neq}_{azaspirane} < \Delta G^{\neq}_{syn} < \Delta G^{\neq}_{anti}$ (Table 2) informed us about the order in which, on heating, these compounds were rotationally 'activated' (Fig. II in SD 3). First, a *local homomeric rotation (topomerisation)* about the C(*s*-triazine)–N(azaspirane) bond occurs, then, in tandem with a *local diastereomeric rotation* about the C(4)(*s*-triazine)–N(exocyclic) bond, to create, finally, a *global diastereomeric rotational motion.* To conclude, this order was parallel with an increase in the solvation of the N-ligands solvation: azaspirane<amino(poly)ol as *syn* N-ligand<amino(poly)ol as *anti* N-ligand.

3.1.2. Analysis of G-0 melamines. rotamerism. Specific NH···OH interactions. Aggregations. When the C-2 chlorine of G-0 dendrons **4a**–**e** was replaced by a bulky, basic and strong electron donating piperazine *A* motif to provide melamines **5**–**7**, three features were expected (i) a diminished *s*-triazine ring π-deficiency, (ii) a decreased bond order C(*s*-triazine)–N(exocyclic) and (iii) an augmented basicity of *s*-triazine nitrogens. The data are presented in Table 4 (see Table II in SD 7 for compounds **5a**, **5b**, **7a**, **7b** and **7e**).

At room temperature, on ^{1}H NMR timescales, the signals as broad lines indicative of slow rotational exchange between equally (**5a**, **5b**) or unequally (**6a**–**e**, **7a**, **7b**, **7e**) populated sites were observed. On heating at 353 K, all G-0 melamines reached *fast exchange* (*freely rotating*) (Fig. IVa and c in SD 6). No *pseudo freely rotating* situation was observed.

On ^{13}C NMR timescales, at room temperature, however, we observed something different.In serinolic melamines **6a**–**c**, the C(4)–N(azaspirane) bonds were axes of prodiastereomerism because azaspiranic carbons C-α′, -α″ were found to be diastereotopic.[22e] This was the same for related compounds **5a**, **5b**, **7a** and **7b**. In compounds **6b** and **6c**, this rotamerism could be additionally located about the C(2)–N(piperazine *A*) bonds, with the piperazine carbons C-β′, -β″ also being diastereotopic. The corresponding anisochrony had about the same magnitude as we had encountered in the more π-deficient *s*-triazines, **4a**–**c**-*anti* (Table 2; Fig. IVb in SD 6). For 'mono-hydroxylated' melamines **6d** and **6e**, the above rotational prodiastereomerism could only be presumed because no $\Delta\delta_C$ diastereotopicity was detected due to broad signals for C-α (azaspirane) and C-β (piperazine *A*). In all our G-0 melamines, their (poly)olic counterpart displayed, clearly, only a single ^{13}C environment as one set of sharp signals for all positions. Hence, the rotational diastereomerism about the C(6)–N(exocyclic) axes existed, most likely, as a unique orientation.

In spite of their different construction, all G-0 melamines had TG values far less negative than their more π-deficient precursors **4a**–**e**. In compounds **6a**–**c**, TGs >−4 ppb/K were indicative of serinolic NH···OH and NH···N(*s*-triazine) internal hydrogen bonding. This reached a maximum in the case of TRIS derivative **6c** (TG=−1.45 ppb/K). This affinity was not dependent on the melamine structure. For example, TGs in serinolic series **5**–**7a** and **5**–**7b** were almost the same, **5a** (−2.55), **6a** (−2.73), **7a** (−2.71) or even identical in **5**–**7b** (all −2.36). In contrast, as in series **4a**–**e**, for the 'mono-hydroxylated' **6d** and **6e** of series **6a**–**e**, the intramolecular hydrogen bonding was the weakest (TG=−4.72 and −3.80, respectively).

Next, in melamines **6a** and **6b**, each of them having two peripheral geminal hydroxymethyl units, the OH groups appeared to be involved in an additional dynamic relationship (Scheme 4), a fast acid–base intermolecular exchange with piperazine *A*>NH linker, $>C(CH_2OH)_2 \rightleftarrows HN<A$.

In the ^{1}H NMR spectra of **6a** and **6b**, these ^{1}H signals were quite difficult to locate due to a unique and very large singlet mediating the two different environments (Fig. IVa in SD 6). Moreover, upon heating, this situation remained unchanged up to 353 K (Fig. IVc in SD 6). We believe that, in solution, melamines **6a** and **6b** formed molecular aggregates.

In the geminal 'tris-hydroxylated' melamine **6c**, we did not detect an external proton exchange, presumably because of the competitive internal association of the alcoholic units. The ^{1}H NMR spectrum displayed different peaks for protons $-C(CH_2OH)_3$ and *A*>N*H*. The same was valid for 'mono-hydroxylated' melamines **6d** and **6e**.

Furthermore, in piperazine linker *A* for each of **6a**–**e**, one must observe the downfield δ_C value of carbons C-α with respect to C-β′, -β″. We consider this deshielding to also support the above proton exchange, implying the most basic site, *A*>NH, of these melamines. This deprotonates either the two geminal hydroxyl groups as in **6a** and **6b** or, simply, the traces of water in DMSO-d_6 in the case of **6c**–**e**.

By combining all these outcomes, we concluded that:

(i) Owing to the versatile internal versus external NH/OH relationships of serinolic units of **6a**–**c**, it was their azaspiranic counterpart, still exhibiting C-α′ versus C–α″ diastereotopicity, to undergo restricted rotation about the bond C(*s*-triazine)–N(azaspirane).

(ii) Since the two C(*s*-triazine)–N(serinol or azaspirane) bond orders were, normally, very comparable, we conclude the incidence of electronic factors was unimportant. Therefore, we assigned the rotational prodiastereomerism of azaspirane fragment to vicinal steric hindrance by the adoption of

Table 4
Rotational (pro)diastereomerism of compounds **6a**–**e** as issued from (VT) NMR data

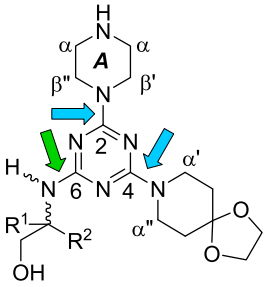

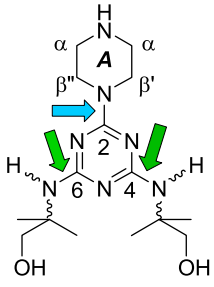

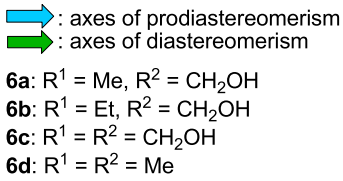

*The piperazine ligand *A* and the *C*-substituted (poly)olic fragment are the references for the descriptors *anti* and *syn*.

No.	δ (ppm)[a], appearance, in [D6]DMSO						TG as $(\Delta\delta_{NH}/\Delta T) \times 10^3$ (ppb/K)
T (K)	NH	*A*>NH	OH	Azaspirane	Piperazine *A*		
				H-α C-α', -α''[b]	H-α C-α	H-β C-β', -β''[b]	
6a 298	5.70 (s)	4.14 (bs)		3.71 (bt)	2.70 (bs)	3.58 (bs)	-2.73
	↓			*41.4 41.1*	45.7	*44.0*	
353	5.55 (s)	3.95 (bs)		3.73 (t)[d]	2.74 (t)	3.61 (t)	
6b 298	5.57 (s)	3.70 (bs)		3.71 (bt)	2.67 (bt)	3.55 (bt)	-2.36
	↓			*41.5 41.1*	45.9	*44.4 44.2*	
353	5.44 (s)	3.73 (bs)		3.73 (t)	2.71 (t)	3.58 (t)	
6c 298	5.68 (s)	3.85 (bs)	4.74 (bs)	3.71 (bs)	3.06 (bs)	3.86 (bs)	-1.45
	↓			*41.7 41.1*	42.9	*40.4 40.0*	
353	5.60 (s)	3.90 (bs)	4.65 (bs)	3.73 (t)	3.08 (bs)	3.89 (bs)	
6d 298	5.84 (s)	3.25 (bs)	4.70 (s)	3.72 (bt)	2.67 (bs)	3.57 (bs)	-4.72
	↓			*41.2*	45.9	*44.3*	
353	5.58 (s)	3.33 (bs)		3.74 (t)	2.71 (t)	3.59 (t)	
6e 303	5.64 (bs)	3.15 (bs)	4.95 (bs)	-	2.66 (bs)	3.55 (bt)	-3.80
	↓				46.0	*44.4*	
353	5.45 (s)	2.95 (bs)	4.65 (bs)	-	2.70 (t)	3.57 (t)	

[a]For **6a-d** on 400 MHz ^{1}H and 100 MHz ^{13}C NMR timescale; for **6e** on 500 MHz ^{1}H and 125 MHz ^{13}C NMR timescale.
[b]*Italicised:* broad signals; diastereotopicity, when observed, was assigned arbitrarily. [d](t) at 353 K as typical triplets with $^3J_{H,H}$ = 5.5-6.5 Hz.

the serinolic group of a prevailing *anti* orientation, as in the series of precursors **4a**–**c**-(*a*). Once more, we deduced that this spatial arrangement best exposed the NH and OH groups to the observed intra- versus extramolecular interactions.

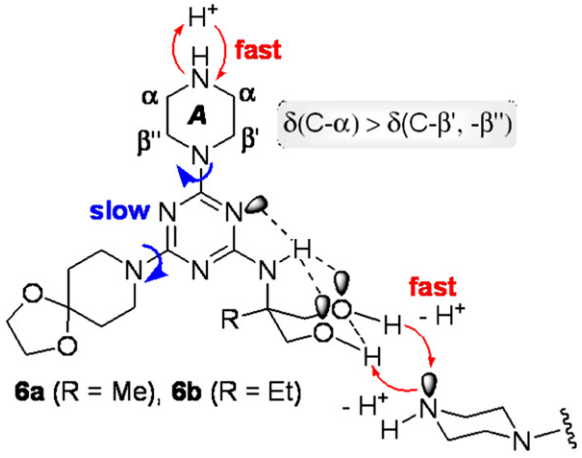

Scheme 4.

3.1.3. G-1 and G-2 dendritic compounds. From peripheral, via internal, to frontier rotamerism. First of all, 2D DOSY ^{1}H NMR[26] of our G-2 dendritic melamines **10** and **11** confirmed their macromolecular nature (Fig. VIa–e in SD 8 and Fig. VIIa–f in SD 9). Table 5 reports the diffusion coefficients (*D*) together with the corresponding hydrodynamic diameters, d_H.

Hydrodynamic diameters d_H were calculated from the hydrodynamic radii r_H by applying the well-known Stokes–Einstein equation (Eq. 1).

$$D = \frac{kT}{6\pi\eta r_H} \times 10^{-9} \quad (1)$$

where *k* is the Boltzmann's constant (1.38×10^{-23} J/K), η is the dynamic viscosity (2.00×10^{-3} kg m^{-1} s^{-1}) of DMSO at *T* (298 K) and r_H (nm) is the hydrodynamic radius.

We then analysed the dynamic rotational behaviour of the dendrimers based on two concepts:

(i) Dynamic behaviour around C(*s*-triazine T-0)–N[azaspirane, amino(poly)ol] bonds (henceforth called '*peripheral rotamerism*')
(ii) Dynamic behaviour around C(*s*-triazine T-0, -1, -2)–N(piperazine *A* or *B*, piperidine) bonds (henceforth called '*internal rotamerism*')

Table 5
Diffusion coefficients (D) and hydrodynamic diameters (d_H) of compounds **10** and **11**

No.	D[a] (μm²/s)	d_H (nm)
10a	80.9	2.70
10b	73.1	2.99
10c	101.4	2.16
10d	79.2	2.76
10e	75.8	2.89
11a	65.6	3.34
11b	61.0	3.59
11c	53.8	4.07[b]
11d	72.6	3.01
11e	61.1	3.58

[a] At 298 K as 5 mM in DMSO-d_6.
[b] Identified as a unique macromolecular species in a mixture (Fig. VIId in SD 9).

We exploited our knowledge of G-0 melamines **6a**–**e**, which were seen as 'references structures' with respect to their subsequent dimeric **8**, **9**, tetrameric **10** and octameric **11** angularly coupled homologues.

At room temperature, all compounds **8**–**11** exhibited broad ^{1}H NMR resonances that were consistent with slow rotational processes. By increasing the temperature at 353–363 K, they displayed convincing line shapes, in accord with an acquired mobility (Fig. Va and b in SD 10).

Furthermore, inspection of temperature gradients showed values, which were not too sensitive to the increase of molecular dimension (Chart 4; Table III in SD 11).

In the 'Methylserinolic' series **6**–**11a**, all compounds had identical TGs (−2.73 ppb/K); it is our contention that this was so because they kept the same kind of intramolecular NH···OH association. One discrepancy was observed in the related 'Ethylserinolic' series **6**–**11b** with TG values of −2.36 ppb/K in **6b**, **9b** and **10b** but a TG of −1.45 ppb/K for chlorodendron **8b**. However, dendrimers **11a** and **11b** had an identical TG, −2.73 ppb/K. As expected, TRIS based derivatives **8**–**10c** had the least negative TGs. As in series **8**–**11b**, the NH groups had the most internal association in chlorodendron **8c** (TG=−0.91 ppb/K) followed by a TG of −1.38 ppb/K in compounds **9c** and **10c** (−1.45 ppb/K in the 'reference' **6c**). Like G-0 melamines **6d** and **6e**, in series **8**–**11d** and **8**–**11e**, the lone hydroxyl group/aminoalcohol peripheral unit was least available to bind to the neighbouring NH proton. In these series we found the most negative TGs. Illustratively, dendrimer **11d** had the most NH···DMSO solvation (TG=−5.27 ppb/K).

Differently than their building-blocks G-0 **6a** and **6b** (Table 4, Scheme 4), G-1 melamines **9a** and **9b** formed no external aggregates of type $>C(CH_2OH)_2 \rightleftarrows HN<B$ since individual δ_H values were found for the depicted 'mobile' protons (Fig. Vb in SD 10).

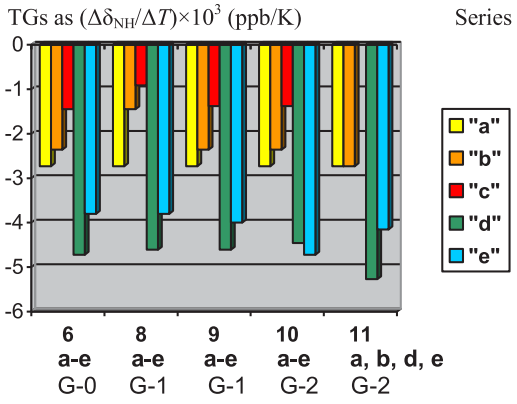

Chart 4. Temperature gradients (TGs) of compounds **6**, **8**–**11**.

On the whole, all these ^{1}H NMR data did not furnish significant differences concerning the *peripheral rotamerism* in **8**–**11** versus their 'monomeric' precursors **6**.

Next, by means of a 'model compound',[14] the symmetrically *N*,*N*′-disubstituted 2-chlorodiamino-*s*-triazine **1a**, we attempted to 'simulate' the *internal rotamerism* in chlorodendrons G-1, -2 **8a**–**e** and **10a**–**e**. The (VT) NMR analysis of compound **1a** is summarised in Chart 5.[11b]

Due to the presence of a great number of anisochronous α-methylenic CH_2–N groups in **8a**–**e** and **10a**–**e**, we extrapolated cautiously the results in the case of **1a**. $\Delta G^{\neq}$ of **1a** was very similar to that of double azaspiranic *s*-triazine **2a** ($\Delta G^{\neq}$=66.11±0.25 kJ/mol, Chart 2). That is, $\Delta G^{\neq}$ of **1a** provided a rough sketch for the operation of rotational behaviour around C(*s*-triazine, T-1, -2)–N(piperazine *A* or *B*) bonds in **8a**–**e** and **10a**–**e**. Therefore, we assumed that the *local* rotational 'activation' about C(*s*-triazine)–N(azaspirane, piperazine, piperidine) bonds required not more than ~67 kJ/mol, i.e., in the situation when the most π-deficient motif, 2-chloro-4,6-bis(piperazine-1-yl)-*s*-triazine, was incorporated by our G-1, -2 dendritic compounds.

By contrast, ^{13}C NMR data were much more informative. Thus, at room temperature, on ^{13}C NMR timescales and for all relevant aspects of series **8**–**11a**–**d**, the C(*s*-triazine T-0)–N(azaspirane) bonds still remained peripheral axes of prodiastereomerism. This, at any rate, was our finding on the basis of azaspiranic carbons C-α′, -α″, which were found to be diastereotopic (Chart 6; Fig. VIII in SD 12). Their $\Delta\delta_C$ values had similar size to those established for G-0 precursors **6a**–**d** (Table 4).

We already mentioned that G-1 melamines **9a** and **9b** did not aggregate in solution. Nevertheless, as in G-0 melamines **6a**–**e** (Table 4, Scheme 4), in the piperazine *B* rings of series **9a**–**e**, we observed a downfield shift of their α-carbons. Therefore, our assignment was the same as that in the case of **6a**-**e**, namely a fast proton interchange, this time as $B>NH \rightleftarrows HOH$ (Chart 6).

Furthermore, compounds **10a**-**e**, **11a**, **11b** and **11e** were investigated by QC ^{13}C NMR spectroscopy (Fig. IX in SD 13; Fig. Xa–d in SD 14). Now, we found on the one hand that QC ^{13}C calculation of **10a**–**e** was routine; no difference between G-2 chlorodendrons of series **10a**–**e** was noticed. On the other hand, in G-2 dendritic dimers **11**, combined QC ^{13}C NMR and (VT) ^{1}H NMR data revealed perturbation of the magnetic environment of the 4,4′-bipiperidine central linker (Chart 7).

This perturbation consisted of deshielding of the ^{13}C positions 2, 2′, 6, 6′ and shielding of the ^{1}H positions 3, 3′, 4, 4′, 5, 5′ in **11e** with respect to **11a**, **11b** and **11d**. Since the constitution of the dendritic networks in series **11** was identical except the peripheral units, our assumption was that it was the peripheral units to which we should look to account for this difference.

The answer we reached was provided, unexpectedly, by the QC ^{13}C calculation (Schemes 5 and 6, Fig. 1). Firstly, the integration of ^{13}C signals in **11e** was in agreement, in both *s*-triazines rings T-2, -2′, with the same normal anisochrony, two types of C-nuclei as six carbons in a 4:2 ratio, δ_C [(C-4)≡(C-4′)≡(C-6)≡(C-6′)]≠δ_C[(C-2)≡(C-2′)]. Therefore, in **11e**, it was credible that, regardless any rotational orientation (*s*–*s*), (*a*–*s*) or (*a*–*a*) of its peripheral *N*-ligands, internal topomerisations of branches $R^{2a(')} \rightleftarrows R^{2b(')}$, $R^{1a(')} \rightleftarrows R^{1b(')}$ (Scheme 5) with respect to the axes of prodiastereomerism C(*s*-triazine)–N(piperazine, piperidine) occurred randomly.

To our surprise, in compounds **11a** and **11b**, calculation discovered three types of C-nuclei for the six *s*-triazine carbons in a 2:2:2 ratios, i.e., the same three different 'unpaired' carbons for each 'monomeric half' of the dendrimer. We normally located them in the 'unpaired' T-2, -2′ *s*-triazine rings (Scheme 5).

On the ^{13}C NMR timescale, just two statistically *planar formulations* corroborate this assignment (Scheme 6). Firstly, isochronous *s*-triazines′ T-2$^{(')}$ C-nuclei 4↔6′ and 4′↔6 or 4↔4′

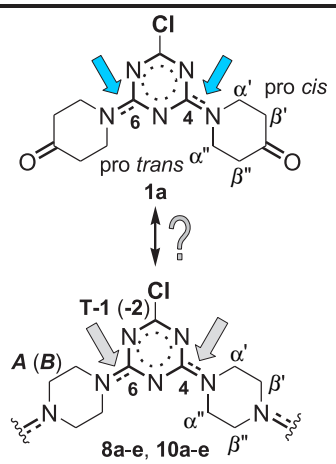

(VT) ^{1}H NMR data of compound **1a** as δ_H (ppm), appearance, in [D$_6$]DMSO on 500 MHz timescale

→ *Frozen* (293 K)			
1st "internal clock" [22a]		2nd "internal clock" [22a]	
H-α'	H-α"	H-β'	H-β"
4.03 (t)	3.99 (t)	2.47 (t)	2.44 (t)
Slowly rotating (coalescences, T_c K)			
4.02 (313)		2.46 (308)	
↻ *Freely rotating (Fast exchange)* (343 K)			
4.03 (t)		2.48 (t)	
$\Delta G^{\neq}_{313}$ = 66.91 kJ/mol[a]		$\Delta G^{\neq}_{308}$ = 66.53 kJ/mol[a]	
$\Delta G^{\neq}$ = 66.72 ± 0.19 kJ/mol			
δ_C (ppm) in [D$_6$]DMSO on 125 MHz timescale (293 K)			
C-α'	C-α"	C-β'	C-β"	C-4, -6
41.7	41.6	40.1	39.9	164.0

[a]Eyring algorithm was used.[22b, 22c]

Chart 5. Rotational prodiastereomerism of 'model compound' **1a** as issued from (VT) ^{1}H NMR data.

and 6↔6′ were also homotopic because rotamers **11a**-, **11b**-[(*a*–*s*)|(*s*–*a*)][§] were C_{2S} whereas **11a**-, **11b**-[(*s*-*a*)|(*s*-*a*)] were C_i symmetric. Secondly, only in **11a** and **11b** were there lateral branches R^{1a} and $R^{1a'}$ (Scheme 5) that had to accommodate two different bulky peripheral units. Consequently, the depicted steric orientation, designed simply as 'serinol against serinol', we saw the preferred one. Furthermore, this allowed multiple hydrogen bindings. These binding we might term an 'inner dendritic communication', which thus created a *pseudo*-macrocyclic cavity. Hence, we have $R^{1a} \neq R^{1b}$ and $R^{1a'} \neq R^{1b'}$. That is, in spite of an exacerbated C(*s*-triazine)–N(exocyclic) rotational diastereomerism of **11a** and **11b**, only two of its locations were relevant: the *internal* one, around bonds C[*s*-triazine T-0$^{(')}$]–N[piperazine $A^{(')}$], in tandem with the *peripheral* one, in respect of C[*s*-triazine T-0$^{(')}$]–N(serinol **A** or **B**) (Scheme 5). They generated the two depicted dendritic rotamers for which inclusion aptitudes as an '*open gates*'⇄'*closed gates (in–out)*' process should be anticipated. We have termed this novel behaviour '*frontier rotamerism*'. Since the two 'monomeric halves' are homomorphic, the simplest way by which the two dendritic rotamers can interchange, [(*a*–*s*)|(*s*–*a*)]⇄[(*s*–*a*)|(*s*–*a*)], is the rotation of a single 'monomeric half' about the C-2$^{(')}$ [*s*-triazine T-2$^{(')}$]–N-1$^{(')}$ (4,4′-bipiperidine) bond.

We further observe that a third C_{2S} formulation for **11a**, **11b** as [(*a*–*a*)|(*s*–*s*)] ('*open gates*') (Scheme 6) should, in fact, be ruled out because it involves δ_C [(C-4)≡(C-6)]≠δ_C [(C-4′)≡(C-6′)], hence δ_C (C-2)≠δ_C (C-2′), i.e., four types of *s*-triazines T-2$^{(')}$ C-nuclei as six carbons in a 2:1:1:2 ratio.

Unfortunately, due to its very low solubility in DMSO, dendrimer **11d** did not allow us to obtain a convincing QC ^{13}C NMR spectrum. Therefore, based on its ^{1}H (Fig. IXc in SD 13) and DEPT ^{13}C NMR data (Chart 7), we could only presume that it also belongs to the same family as **11a** and **11b**.

Some account might be given that involved the well-known phenomenon of dendritic backfolding,[3,14] though any such account would have to be carefully adopted. If so, one would want note that, as shown in Table 5, the hydrodynamic diameters d_H (nm) of our dendrimers were almost identical for **11b** (3.59) versus **11e** (3.58). Therefore, if (and this is just an hypothesis) **11a** and **11b** were back-folded, in solution, the *non-planar* resulting dendritic rotamers **11a**-, **11b**-[(*a*–*s*)|(*s*–*a*)] against **11a**-, **11b**-[(*s*–*a*)|(*s*–*a*)] were non-chiral (*meso*-form) and chiral, respectively. If so, the relationships between the 2×(1:1:1) 'unpaired' carbons become: C-4 against C-6′ and C-4′ against C-6 are enantiotopic in *meso*-**11a**-, **11b**-[(*a*–*s*)|(*s*–*a*)] meanwhile, in chiral **11a**-, **11b**-[(*s*–*a*)|(*s*–*a*)], C-4 against C-4′ and C-6 against C-6′ remain homotopic.

3.2. Analysis in solid state by AFM imaging

Given the above, it made sense to subject compounds **11b**, **11d** and **11e** to structural analysis in the solid state. We did this by the technique of AFM (atomic force microscopy), a method the rarely mentioned in the field of dendritic melamines.[5c] AFM can provide new evidence about the shape and the size of dendritic particles or aggregates self-assembled in adsorbed coating films on solid surfaces.[3,27] There are obvious applications in nano-science. However, it must be noted that morphologies (aggregates) observed by AFM may be rather different to those present in solution as a consequence of drying and surface effects.

Dendrimers **11b**, **11d** and **11e** were self-assembled on mica, as solid support, by their adsorption from a 1 mM organic solution. Under controlled conditions, they provided coating films at saturation of the solid surface. These adsorbed films were characterised by AFM operating in tapping mode (TM).

The results of our imaging process are shown in Figs. 2–4. They show that our compounds strongly adsorbed on mica in large aggregates (islands and clusters). These aggregates were of globular shape and relatively uniform size, the adsorbed films being roughly monodisperse.

Fig. 2 shows AFM images of dendrimer **11e**; we see many well-defined globular particles randomly adsorbed on mica. These particles appear to be substantially uniform in size, with an average lateral dimension of about 60±5 nm, indicating that the adsorbed film was rather monodisperse. Nevertheless, there do appear to be a few larger aggregates, of dimensions up to 100 nm. Such images show, furthermore, that dendrimer particles of **11e** were apparently made from supramolecular nano clusters, self-assembled within the coating layer of slightly low surface roughness, given by rms (defined by the root mean square of the height distribution) value on scanned area, of about 9±2 nm.

The AFM experiments, performed with compound **11b** (Fig. 3), also support the hypothesis of the formation of a globular morphology on mica at the adsorption time of 1 h. This phenomenon

§ Symbol '|' designs the peripheral 'frontier' between the two 'monomeric halves' of the dendrimer.

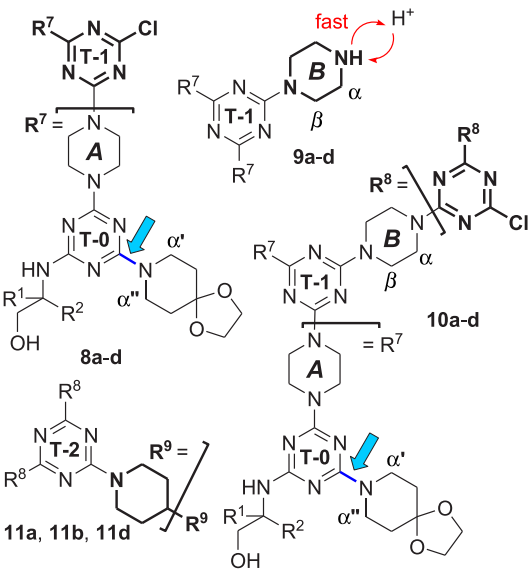

No.	δ_C (ppm)[a] Azaspirane C-α',[b] C-α"	Piperazine *B* C-α	C-β
8a	*41.4*,[c] *41.1*	-	
8b	*41.6*, *41.2*	-	
8c	*41.7*, *41.2*	-	
8d	*41.4*, *41.0*	-	
9a	*41.4*, *41.1*	45.6	43.8
9b	*41.6*, *41.0*	45.3	43.4
9c	*41.6*, *41.1*	45.0	*43.2*
9d	*41.5*, *41.0*	44.1	*43.1*
10a	*41.1*	43.5	43.1
10b	*41.6*, *41.0*	43.4	43.1
10c	*41.6*, *41.1*	43.5	43.3
10d	*41.4*, *41.0*	43.5	43.1
11a	*41.4*, *41.1*	43.1	
11b	*41.6*	43.1	
11d	41.0	43.1	

[a]On 100 MHz ^{13}C NMR timescale for **8a-c**, **9a**, **9b** and **10a**; on 125 MHz ^{13}C NMR timescale for **8d**, **9c**, **9d**, **10b**, **10c**, **11a**, **11b** and **11d**. [b]Arbitrarily assigned **α'** *vs.* **α"**. [c]*Italicised* data: broad signals.

Chart 6. Peripheral rotamerism of compounds **8**–**11** as issued from (QC) ^{13}C NMR data.

leads, in turn, to the surface saturation with an average lateral size of about 46±4 nm for dendrimer particles. The resulting coating film of dendrimer **11b** shows a rather low roughness of about 11±3 nm.

These morphological features were similar to those observed in the case of compound **11d** (Fig. 4). Specifically, the AFM images clearly showed adsorbed aggregates of compound **11d** with an average lateral size of about 37±4 nm and a very low roughness of about 6±2 nm.

Comparatively, one can clearly observe that globules of dendrimer **11e** (Fig. 2) were wider (lateral size of particles between 56 and 85 nm) than those of both **11b** (width from 30 to 65 nm, Fig. 3) and **11d** (width from 24 to 43 nm, Fig. 4) for each coating film obtained after an adsorption time of 1 h on mica. This is not surprising as the aggregates of dendritic molecules are expected to be larger for dendrimer **11e** than for the corresponding aggregates of dendrimers **11b** and **11d** adsorbed onto the mica surface, in substantial agreement with their molecular structure and with

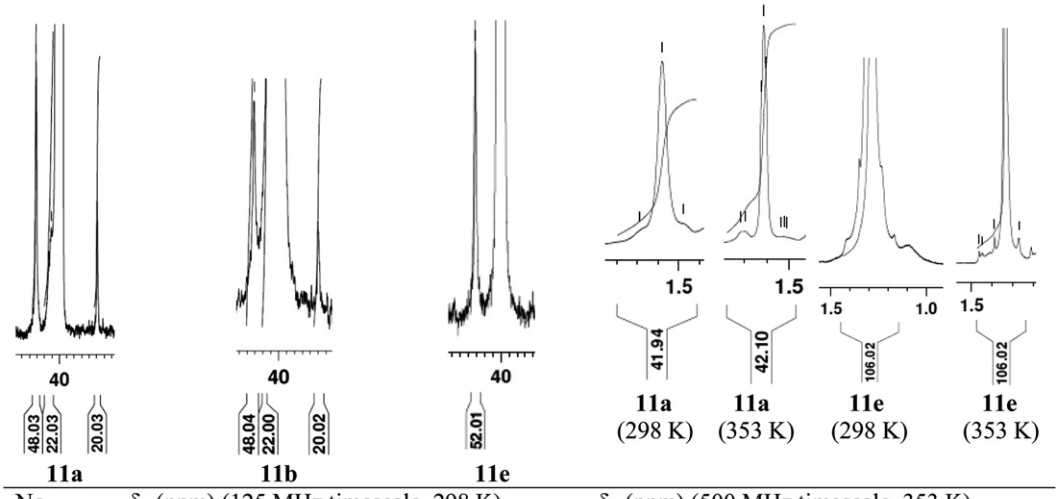

No.	δ_C (ppm) (125 MHz timescale, 298 K) 2, 2', 6, 6'[a]	4, 4'[a]	3, 3', 5, 5'[b]	δ_H (ppm) (500 MHz timescale, 353 K) 2, 2', 6, 6'[c]	4, 4'[d]	3, 3', 5, 5'[d]
11a	41.1, 41.4		34.9	3.77-3.72	1.51-1.72	
11b	41.6		35.0	3.75-3.70	1.61	
11d	41.0		34.9	3.75-3.71	1.60	
11e	43.1	Not detected		3.72-3.71	1.27-1.46	

[a]Together with 16C (α-azaspiranic) in **11a** and **11b** but together with 48C (piperazines *A* + *B*) in **11e**; [b]Together with 16C (β-azaspiranic) in **11a** and **11b**; [c]Together with 96H (piperazines *A* + *B*) and 32H (α-azaspiranic) in **11a**, **11b** and **11d** but together with 32H (piperazines *B*) in **11e**; [d]Together with 32H (β-azaspiranic) in **11a**, **11b** and **11d** but together with with 96H (methyl) in **11e**.

Chart 7. Comparative details from NMR spectra (5 mM in DMSO-d_6) of compounds **11a**, **11b** and **11d** with respect to **11e** in the 4,4′-bipiperidine central linker zone.

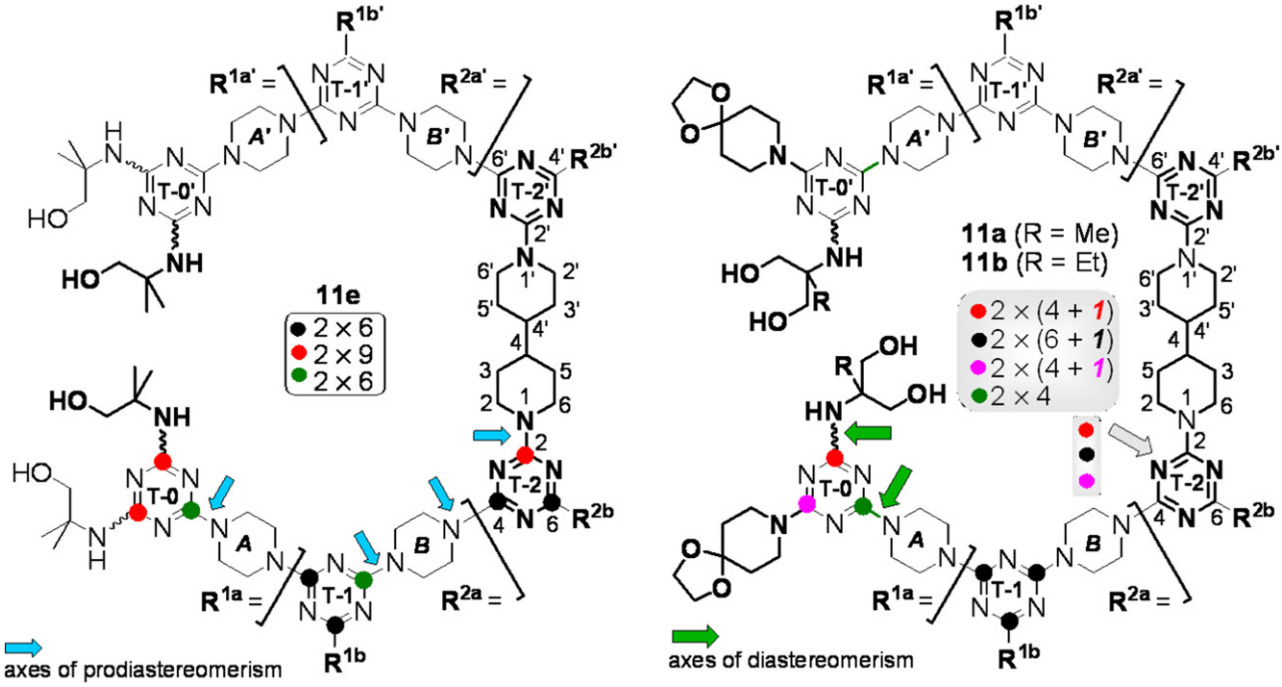

Scheme 5.

the different kind of interaction with the surrounding medium. The surface roughness, rms, on scanned area of 1 μm×1 μm, indicated that dendritic films were almost flat, with compound **11e** having an rms value of 9±2 nm, **11b** an rms of 11±3 nm and **11d** an rms of 6±2 nm. We can speculate, with some plausibility, on the origin of such flattened dendritic aggregates. It might be attributed to their ready adsorption on hydrophilic mica as a consequence of the hydroxyl *termini* functionalities on all investigated compounds.

The resulting adsorbed species self-assembled in rather compact networks and this can be observed across all the AFM images. They exposed a compact packing of individual dendrimer aggregates inside their coating film. Our macromolecules strongly interacted with the mica surface primarily through hydrophilic interactions of their peripheral OH groups in a natural tandem with the hydrophilic nature of mica.

To conclude, we assume that the morphology of adsorbed layered networks was assisted by the nature of the self-assembled structure of our dendrimers.[27c] Considering rms values, compound **11d** was adsorbed on mica in a rather flattened nanostructured film when compared to compounds **11e** and **11b**. The slight differentiation probably originates from the different interaction among particles and with the organic solvents present during the adsorption of dendrimers on mica surface, as well as with the mica surface.

4. Conclusions

(i) We report the seven-step convergent synthesis of a new family of dimeric G-2 dendritic melamines with a commercial amino(poly)ol (C-2-substituted serinols or 2-amino-2-methylpropanol)—ethylene ketal of 4-piperidone tandem as peripheral units. This was effected by iterative chemoselective aminations of cyanuric chloride. This synthesis occurred with a range of yields from satisfactory to good, except the case of TRIS, for which the proposed chemistry was applicable only up to the G-2 chlorodendron stage. The same strategy was also valid for 2-amino-2-methylpropanol as a unique peripheral unit.

(ii) The structural analysis of our amino-*s*-triazines was based on combined NMR methods. This was so because of the main focus on the restricted rotations phenomena around the C(*s*-triazine)—N(exocyclic) partial double bonds. For G-0 chlorodendrons, canonical algorithms (Eyring, Gutowski-Holm and Shanan-Atidi) provided pertinent kinetic results. The dynamic behaviour of our compounds (rotamerism, acid—base interchange and aggregation) was dictated, mainly, by solvation effects involving the amino(poly)olic units. Their G-0→G-2 complexity did not seem to affect this.

(iii) The ethylene ketal of 4-piperidone counterpart was the most relevant marker for the existence of rotamerism because the bond C(*s*-triazine)—N(azaspirane) was, continuously, an axis of prodiastereomerism.

This includes G-1, -2 dendritic compounds ('*peripheral rotamerism*').

(iv) Starting from G-1 dendrons, their '*internal rotamerism*' could be approximated by structural simulation. Overall, the $\Delta G^{\neq}$ rotational barriers in all our melamines did not exceed 67 kJ/mol.

(v) If the peripheral units of G-2 dimeric melamines were the tandem (*Methyl-* or *Ethylserinol*)-(ethylene ketal of 4-piperidone), a new type of '*frontier rotamerism*' dynamic '*open gates*⇄*closed gates*' behaviour was observed, and this affected the adjacent branches subsequent to dendritic dimerisation.

(vi) Comparative AFM investigations showed that our G-2 dendritic melamines were self-assembled globular structures, which exist as monodispersed films on mica. Nevertheless, globules of the dendritic melamine with peripheral 2-methyl-2-propanol units were thicker and wider than those obtained from the corresponding analogues possessing the *termini* tandem serinol-ethylene ketal of 4-piperidone.

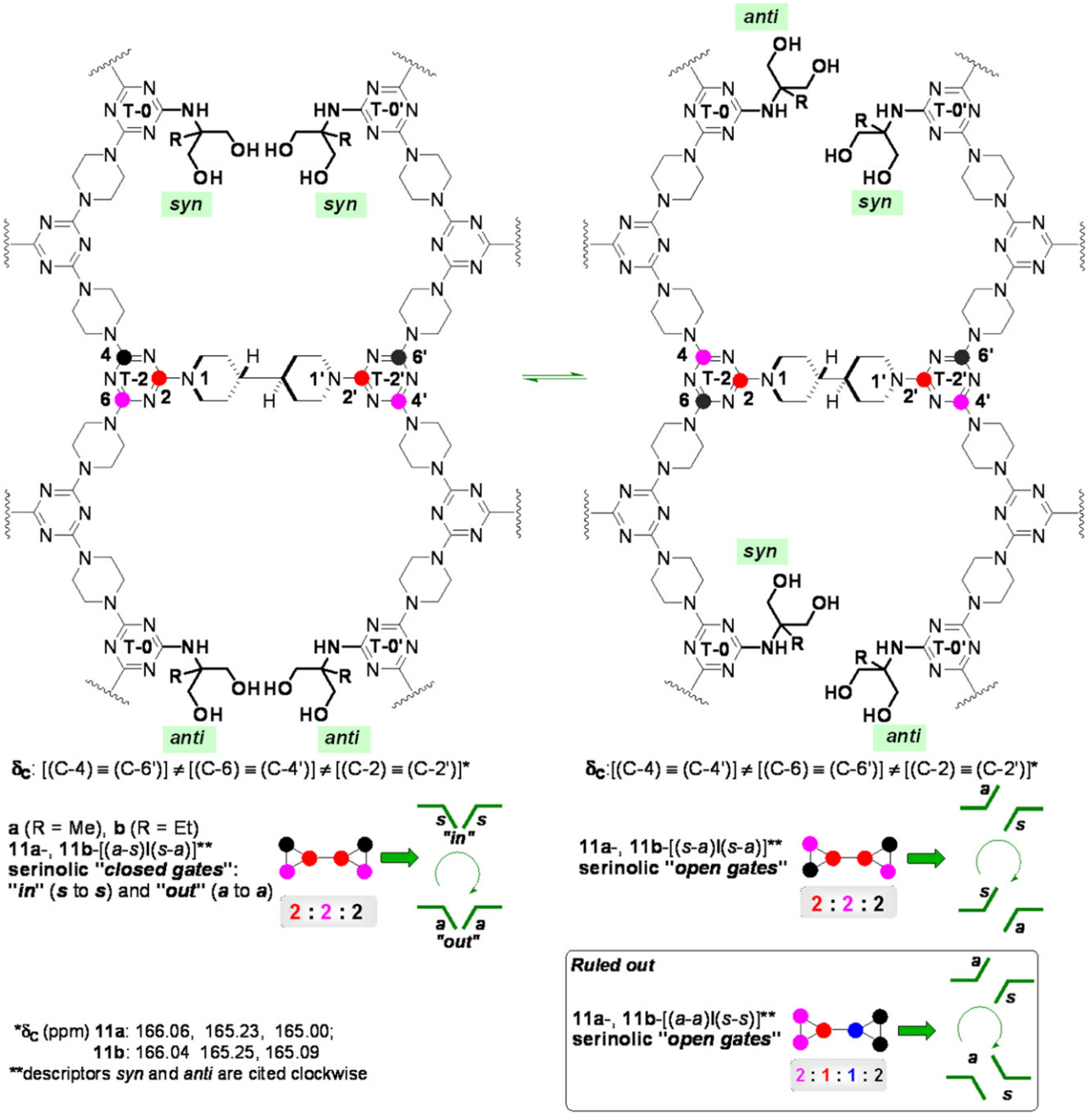

Scheme 6.

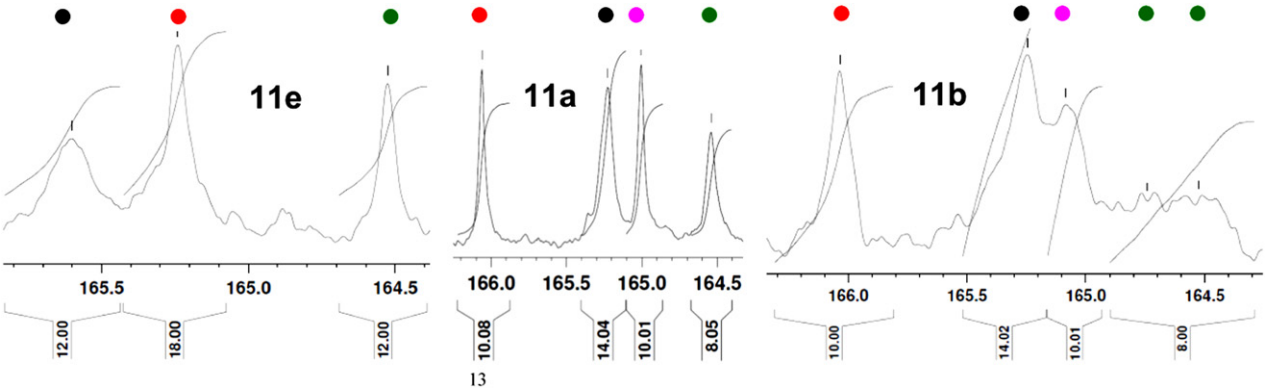

Fig. 1. Comparative details from QC ^{13}C NMR spectra (125 MHz timescale, 5 mM in DMSO-d_6, 298 K) of compounds **11e**, **11a** and **11b** in the *s*-triazines' zone.

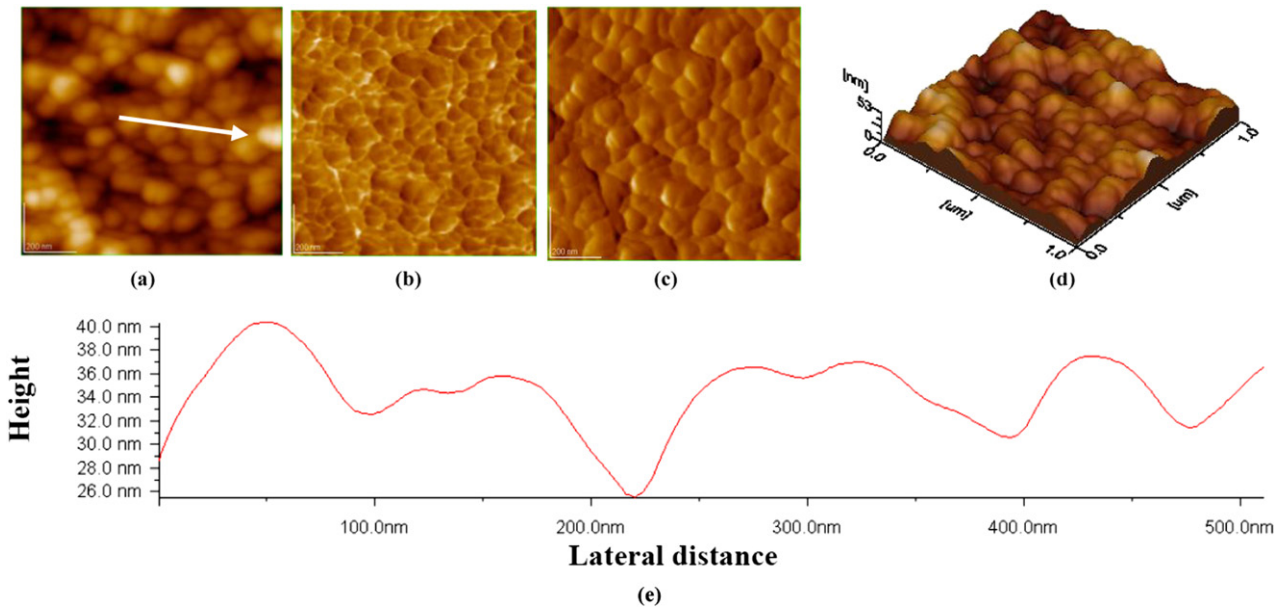

Fig. 2. AFM images for compound **11e** adsorbed for one hour on mica from 1 mM DMSO solution; (a): 2D topography; (b): phase image; (c): amplitude image; (d): 3D topography; (e): profile of the cross section along the arrow in panel (a). Scanned area of 1 μm×1 μm. Surface roughness given by root mean square (rms) on scanned area is about 9 nm (±2 nm). The standard deviation is denoted in parentheses.

5. Experimental section

5.1. General

Melting points are uncorrected; they were carried out on ELECTROTHERMAL® instrument. Conventional NMR spectra were recorded on a Bruker® AM 300 instrument operating at 300 and 75 MHz for ^{1}H and ^{13}C nuclei, respectively. (VT) NMR spectra and related experiments were recorded either on a Bruker® AM 400 instrument operating at 400 and 100 MHz for ^{1}H and ^{13}C nuclei or on a Bruker® AM 500 instrument operating at 500 and 125 MHz for ^{1}H and ^{13}C nuclei, respectively. In these last instruments, NMR spectra were measured in anhydrous commercially DMSO-d_6 as one sample/75 μml bottle. All chemical shifts (δ values) are given throughout in parts per million (ppm); all homocoupling patterns ($^{n}J_{H,H}$ values) are given throughout in hertz. TLC was performed by using aluminium sheets with silica gel 60 F_{254} (Merck®); column chromatography was conducted on Silica gel Si 60 (40–63 mm, Merck®). IR spectra were performed on a Perkin–Elmer® Paragon FT-IR Spectrometer. Only relevant absorption maxima are listed, throughout, in cm^{-1}. Microanalyses were performed on a Carlo Erba® CHNOS 1160 apparatus. Mass spectra (MS) were recorded as follows: FAB Spectra on a JEOL® AX500 Instrument equipped with a DEC DA 5000 computer and ionisation realised with a FAB JEOL®

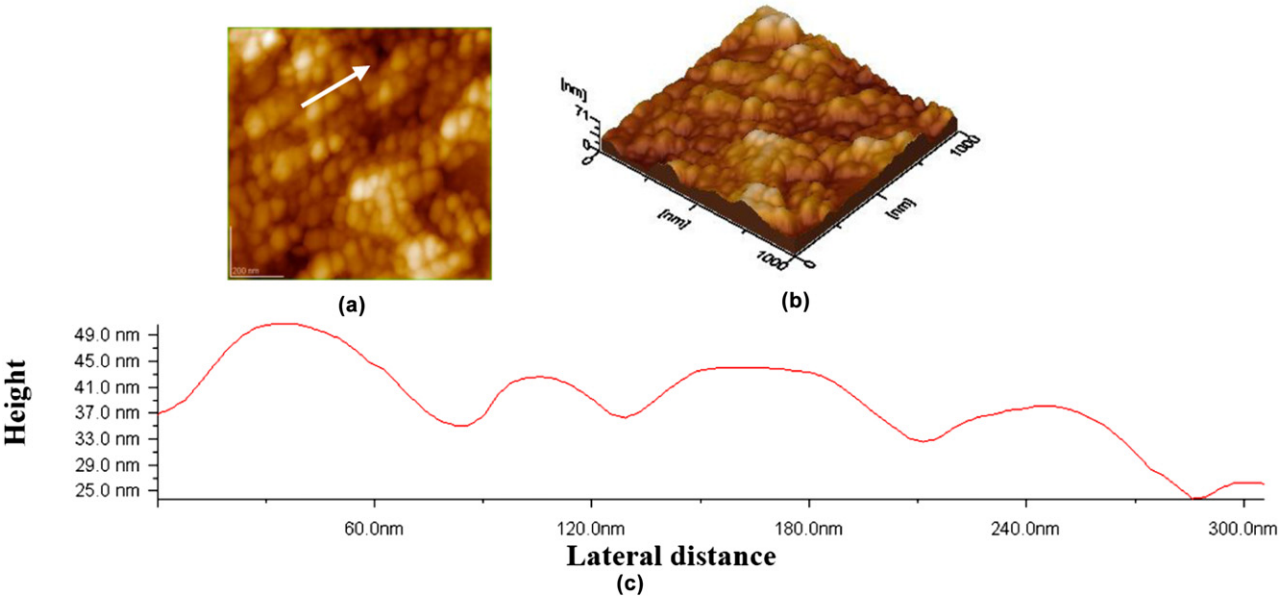

Fig. 3. AFM images of compound **11b** adsorbed for 1 h on mica from 1 mM DMSO solution; (a): 2D topography; (b): 3D topography; (c): profile of the cross section along the arrow in panel (a). Scanned area of 1 μm×1 μm. rms on scanned area is about 11 nm (±3 nm).

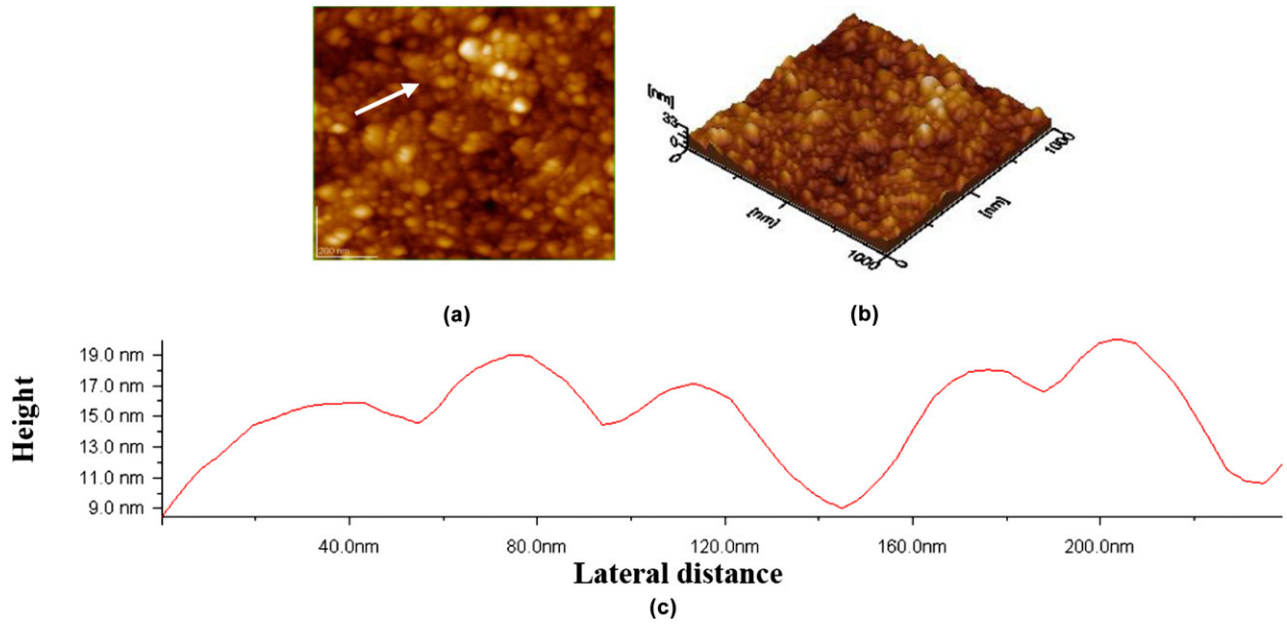

Fig. 4. AFM images of compound **11d** adsorbed for 1 h on mica from 1 mM mixed solution of $CHCl_3$/abs EtOH (3:1, v/v); (a): 2D topography; (b): 3D topography; (c): profile of the cross section along the arrow in panel (a). Scanned area of 1 μm×1 μm. rms on scanned area is around 6 nm (±2 nm).

Cannon (fascicle of Xenon accelerated under 4 kV/10 mA); MALDI spectra on Micromass TOF-SpecE MALDI® Instrument equipped with a time of flight analyser and a nitrogen pulsed laser (337 nm); ESI spectra on a Bruker® Esquire Instrument with ions trapping in electrospray mode. Except DMF, all reagents and solvents were of commercial quality and used as such with no supplementary purification. Only DMF was freshly distilled prior to use.

The synthesis and data of compounds **1a** and **2a** (Scheme 1) we reported, in detail, elsewhere.[11b,13b–d] Complete characterisation of the non-isolated intermediates **3a**–**c** we reported elsewhere.[11b] For the present study, isolation of **3d** was not considered of interest because of the good and reproducible result obtained in the preparation of **4e** (Table 1, entry 4). The synthesis and data of compounds **4a**–**c**, **5a**, **5b**, **7a**, **7b** (Scheme 2) we reported elswhere.[13d] For the present discussion see Tables 1, 2, and 4, Table II in SD 7, Fig. I (compound **4b**) in SD 2, Fig. II (compound **4b** in SD 3) and Fig. IVa–c (compound **6a**) in SD 6.

In the NMR descriptions, some specific abbreviations were used: 'br t' (broad triplet), 'br d' (broad doublet), 'br m' (broad multiplet), 'ot' (overlapped triplet), '*A*' or '*B*' (piperazine linkers), T-0, -1, -2 (*s*-triazine, branch cells), **A**–**D** [amino(poly)ol, peripheral units], a.s. (azaspirane) and bip (4,4′-bipiperidine, central linker) (Schemes 2 and 3).

*5.1.1. Typical procedure for the synthesis of compounds **4a**–**d**. Preparation of compound **4d** (Scheme 3).* To anhyd K_2CO_3 (1.15 g, 8.30 mmol) suspended in a dry THF (75 mL) solution containing cyanuric chloride (1.53 g, 8.30 mmol), solid 2-amino-2-methylpropanol (0.740 g, 8.30 mmol) was added, at room temperature, with vigorous stirring. The stirred suspension was kept at room temperature for an additional 24 h. when TLC monitoring (toluene/*i*-PrOH 2:1) indicated formation of the intermediate **3d** as a single major spot. Water (7.50 mL) and anhyd K_2CO_3 (2.30 g, 16.60 mmol) were added and the reaction mixture was cooled at −10 °C (−15 °C). At this temperature, solid 1,4-dioxa-8-azaspiro [4.5]decane hydrochloride **2** (1.49 g, 8.30 mmol) was added portionwise (five equal portions as 0.298 g/portion each 90 min). The reaction mixture was kept at −10 °C (−15 °C) for an additional 36 h then allowed to reach room temperature very slowly. After filtering minerals, water (50 mL) and chloroform (100 mL) were added to the organic solution. The aqueous layer was extracted with chloroform (2×35 mL) and the combined organic layer was washed with water (3×35 mL) to neutrality. After drying over anhyd Na_2SO_4, the organic solution was evaporated under reduced pressure to dryness to provide 2.88 g crude product, which was crystallised from boiling ethanol (6 mL) to yield, after standing for 24 h at −18 °C, the pure title compound **4d** (2.42 g, 85% yield with respect to cyanuric chloride).

*5.1.1.1. 2-Chloro-6-{[1-hydroxy-2-(methyl)prop-2-yl]amino}-4-(1,4-dioxa-8-azaspiro[4.5]decan-8-yl)-s-triazine (**4d**).* White crystalline solid, mp 143.8–144.5 °C (EtOH). Found: C, 49.11; H, 6.77; N, 20.22%. $C_{14}H_{22}ClN_5O_3$ (343.14) requires C, 48.91; H, 6.45; N, 20.37%; R_f (75% Ligroin/acetone) 0.52; ν_{max} (KBr) 3430, 3301, 2990, 2960, 2931, 2878, 1573, 1537, 1504, 1453, 1406, 1362, 1308, 1232, 1149, 1120, 1188, 1088, 1056, 1028, 948, 889, 800, 704, 658, 622 cm^{-1}; δ_H (400 MHz, DMSO-d_6, 353 K) 1.31 (6H, s, Me), 1.66 (4H, t, *J* 5.8 Hz, H-6, -10, a.s.), 3.49 (2H, s, CH_2OH), 3.78, 77 (4H, ot, *J* 5.8 Hz, H-7, -9, a.s.), 3.93 (4H, s, H-2, -3, a.s.), 4.56 (1H, br s, OH), 6.75 (1H, br s, NH) ppm; δ_C (100 MHz, DEPT, DMSO-d_6, 293 K) 23.9 (Me, *anti*), 24.3 (Me, *syn*), 34.6, 34.8 (C-6, -10, a.s., *anti*, *syn*), 41.4, 41.8, 42.0 (C-7, -9, a.s., *anti*, *syn*), 55.1 (C-2, **D**, *anti*), 55.3 (C-2, **D**, *syn*), 64.3 (C-2, -3, a.s., *syn*), 64.4 (C-2, -3, a.s., *anti*), 67.1 (CH_2OH, *anti*), 67.7 (CH_2OH, *syn*), 106.9 (C-5, a.s., *anti*), 107.0 (C-5, a.s., *syn*), 163.6 (C-4, T-0, *syn*), 164.0 (C-4, T-0, *anti*), 165.0 (C-6, T-0, *anti*), 165.7 (C-6, T-0, *syn*), 168.5 (C-2, T-0, *anti*), 168.6 (C-2, T-0, *syn*) ppm; *m*/*z* (CI positive, 200 eV, *t*-BuH) 400 (M+*i*-BuH−1) (9), 344 (MH^+) (100), 310 (10%).

*5.1.2. Preparation of compound **4e** (Scheme 2).* To anhyd K_2CO_3 (2.76 g, 20.00 mmol) suspended in a cooled (−10 °C) dry THF (75 ml) solution containing cyanuric chloride (1.80 g, 9.76 mmol), 2-amino-2-methylpropanol (1.78 g, 20.00 mmol) as dry THF (25 ml) solution was slowly injected with vigorous stirring. The reaction mixture was allowed to reach room temperature and kept as such for an additional 12 h when TLC monitoring

(toluene/*i*-PrOH 2:1) indicated the formation of **4e** contaminated with the corresponding intermediate the *N*-substituted-2,4-dichloro-*s*-triazine. The reaction mixture was heated to 45 °C for an additional 13 h when TLC monitoring revealed completion of the amination, then cooled at room temperature. Solids were filtered off and well washed with dry THF. The organic filtrate was evaporated under reduced pressure to dryness and the resulting white powder was crystallised from min. boiling ethanol to afford pure **4e** (2.11 g 75% yield with respect to cyanuric chloride).

*5.1.3. 2-Chloro-4,6-bis{[1-hydroxy-2-(methyl)prop-2-yl]amino}-s-triazine (**4e**).* White crystalline solid, mp 171.4–172.3 °C (EtOH). Found: C, 45.77; H, 6.69; N, 23.98%. $C_{11}H_{20}ClN_5O_2$ (289.13) requires C, 45.60; H, 6.96; N, 24.17%; R_f (66% toluene/*i*-PrOH) 0.80; ν_{max} 3370, 3271, 2980, 2839, 1598, 1532, 1474, 1301, 1270, 1196, 1056, 1037, 996, 903, 803, 770, 704, 667, 531, 510 cm^{-1}; δ_H (500 MHz, DMSO-d_6, 353 K) 1.32 (12H, s, Me), 3.48 (4H, d, *J* 6.0 Hz, C*H*$_2$OH), 4.61 (2H, br s, OH), 6.52 (2H, br s, NH) ppm; δ_C (125 MHz, DEPT, DMSO-d_6, 298 K) 24.0, 24.1 (Me), 54.9 (C-2, **D**, *anti*), 55.0, 55.2 (C-2, **D**, *anti*, *syn*), 67.4, 67.9 (CH_2OH, *anti*, *syn*), 67.7 (CH_2OH, *anti*), 164.6, 165.4 (C-4, -6, T-0, *anti*, *syn*), 165.0 (C-4, -6, T-0, *anti*), 167.38 (C-2, T-0, *anti*), 167.43 (C-2, T-0, *anti*, *syn*) ppm; *m*/*z* (DCI positive, 200 eV, *i*-BuH) 346 (M+*i*-BuH−1) (15), 312 (MNa^+) (10), 290 (MH^+) (100), 346 (15), 312 (10), 256 (50), 224 (10), 73 (10%).

*5.1.4. Typical procedure for the synthesis of compounds **6a–e**. Preparation of compound **6e** (Scheme 2).* To anhyd K_2CO_3 (0.96 g, 6.90 mmol) suspended in a dry THF (50 ml) solution containing anhyd piperazine (2.37 g, 27.51 mmol), compound **4e** (2.00 g, 6.90 mmol) as dry THF (20 mL) solution was added portionwise, with vigorous stirring, at room temperature. After addition of each 4 ml of this **4e** THF solution, over 90 min, TLC monitoring established complete consumption of **4e** (toluene/*i*-PrOH 2:1) and formation of the desired **6e** ($CHCl_3$/EtOH 1:1) as major product versus the corresponding 1,4-disubstituted piperazine derivative **7e**. Solids were filtered off and thoroughly washed with dry THF. The organic filtrate was evaporated under reduced pressure to dryness and the solid residue was separated by column chromatography on silica gel to yield, firstly, the side-product **7e** (0.10 g, 5% partial conversion of **4e**, $CHCl_3$/EtOH 1:1), then **6e** (2.01 g, 85% partial conversion of **4e**, EtOH/aq NH_3 25% 9:1).

*5.1.4.1. 1-{4,6-Bis{[1-hydroxy-2-(methyl)prop-2-yl]amino}-s-triazin-2-yl}-piperazine (**6e**).* White crystalline solid, mp 156.5–157.4 °C (column chromatography, EtOH/aq NH_3 25% 9:1). Found: C, 52.88; H, 8.69; N, 29.05%. $C_{15}H_{29}N_7O_2$ (339.24) requires C, 53.08; H, 8.61; N, 28.89%; R_f (90% EtOH/aq NH_3 25%) 0.85; ν_{max} (KBr) 3275, 2968, 2926, 2858, 1597, 1554, 1504, 1441, 1363, 1275, 1242, 1200, 1125, 1050, 811, 614 cm^{-1}; δ_H (500 MHz, DMSO-d_6, 353 K) 1.31 (12H, s, Me), 2.70 (4H, t, *J* 5.0 Hz, H-3, -5, *A*), 2.95 (1H, br s, *A*>NH), 3.44 (4H, s, C*H*$_2$OH), 3.57 (4H, t, *J* 5.0 Hz, H-2, -6, *A*), 4.65 (2H, br s, OH), 5.45 (2H, s, NH) ppm; δ_C (125 MHz, DEPT, DMSO-d_6, 303 K) 24.4 (Me), 44.4 (C-2, -6, *A*), 46.0 (C-3, -5, *A*), 54.1 (C-2, **D**), 69.0 (CH_2OH), 164.4 (C-2, T-0), 165.6 (C-4, -6, T-0) ppm; *m*/*z* (DCI positive, 200 eV, *i*-BuH) 396 (M+*i*-BuH−1) (15), 340 (MH^+) (100), 308 (10), 268 (15), 113 (10), 97 (5), 85 (15), 73 (30%).

*5.1.5. Alternative preparation of compound **7e** (Scheme 2).* To anhyd K_2CO_3 (0.56 g, 4.05 mmol) suspended in a dry THF (50 ml) solution containing anhyd piperazine (0.17 g, 1.97 mmol), compound **4e** (1.16 g, 4.00 mmol) was added with vigorous stirring. The reaction mixture was heated at reflux for 12 h when TLC monitoring (toluene/*i*-PrOH 2:1) showed the formation of **7e** as major component of a mixture containing also the starting **4e** and the intermediate **6e**. THF was replaced by 1,4-dioxane and refluxing was continued for an additional 12 h. After this period, TLC monitoring revealed the presence of **4e** and **6e** in small traces only. Solids were filtered off and thoroughly washed with dry THF. The organic filtrate was evaporated under reduced pressure to dryness. Column chromatography ($CHCl_3$/EtOH 1:1) afforded pure **7e** (0.89 g, 76% yield with respect to piperazine).

*5.1.5.1. 1,4-Bis{4,6-bis{[1-hydroxy-2-(methyl)prop-2-yl]amino}-s-triazin-2-yl}piperazine (**7e**).* White crystalline solid, mp 230–235 °C (column chromatography, $CHCl_3$/EtOH 1:1). Found: C, 52.82; H, 7.89; N, 28.44%. $C_{26}H_{48}N_{12}O_4$ (592.39) requires C, 52.68; H, 8.16; N, 28.36%; R_f (50% $CHCl_3$/EtOH) 0.80; ν_{max} (KBr) 3502, 3419, 3346, 3168, 2964, 2931, 1563, 1494, 1440, 1360, 1281, 1254, 1199, 1167, 1060, 1048, 1017, 994, 898, 833, 809, 743, 595, 563 cm^{-1}; δ_H (500 MHz, DMSO-d_6, 353 K) 1.32 (24H, s, Me), 3.45 (8H, s, *A*), 3.67 (8H, s, C*H*$_2$OH), 4.78 (4H, br s, OH), 5.54 (4H, s, NH) ppm; δ_C (75 MHz, J_{Mod}, DMSO-d_6, 298 K) 20.8, 20.9 (Me), 42.0 (CH_2, *A*), 53.7 (C-2, **D**), 68.4 (CH_2OH), 164.0 (C-2, T-0), 165.0 (C-4, -6, T-0) ppm; *m*/*z* (DCI positive, 200 eV, *i*-BuH) 649 (M+*i*-BuH−1) (5), 593 (MH^+) (100), 562 (10%).

*5.1.6. Typical procedure for the synthesis of compounds **8a–e**. Preparation of compound **8e** (Scheme 3).* To anhyd K_2CO_3 (0.44 g, 3.18 mmol) suspended in a cooled (−10 °C) dry THF (50 ml) solution containing cyanuric chloride (0.29 g, 1.57 mmol) and with vigorous stirring, compound **6e** (1.17 g, 3.45 mmol) as dry THF (25 mL) solution was injected very slowly. The reaction mixture was allowed to warm up to room temperature overnight when TLC monitoring (toluene/*i*-PrOH 2:1) revealed the presence of **8e** as well as the unreacted **6e**. THF was replaced by 1,4-dioxane and the reaction mixture was heated at 90 °C for an additional 11 h when TLC monitoring confirmed the formation of **8e** as major product. At 90 °C, solids were filtered off and thoroughly washed with dry and hot THF. The organic filtrate was evaporated under reduced pressure to dryness and the resulting crude product was triturated at −18 °C with EtOH/Et_2O affording pure **8e** (1.12 g, 90% yield with respect to cyanuric chloride).

*5.1.6.1. 2-Chloro-4,6-bis{4-{6-{[1,3-dihydroxy-2-(methyl)prop-2-yl]amino}-4-(1,4-dioxa-8-azaspiro[4.5]decan-8-yl)-s-triazin-2-yl}-piperazin-1-yl}-s-triazine (**8a**).* Yield 75%; white crystalline solid, mp 241–242 °C (column chromatography, toluene/*i*-PrOH 2:1). Found: C, 50.15; H, 6.29; N, 25.44%. $C_{39}H_{60}ClN_{17}O_8$ (929.45) requires C, 50.34; H, 6.50; N, 25.59%; R_f (66% toluene/*i*-PrOH) 0.72; ν_{max} (KBr) 3398, 2926, 2868, 1563, 1537, 1493, 1440, 1364, 1286, 1257, 1229, 1088, 1000, 978, 807, 661 cm^{-1}; δ_H (400 MHz, DMSO-d_6, 353 K) 1.30 (6H, Me), 1.62 (8H, s, H-6, -10, a.s.), 3.56 (4H, d, *J* 10.0 Hz, C*H*$_2$OH), 3.65 (4H, d, *J* 10.4 Hz, C*H*$_2$OH), 3.76 (24H, s: 8H, H-7, -9, a.s.; 16H, *A*), 3.94 (8H, s, H-2, -3, a.s.), 4.58 (4H, br s, OH), 5.63 (2H, s, NH) ppm; δ_C (100 MHz, DEPT, DMSO-d_6, 298 K) 19.2 (Me), 34.9 (C-6, -10, a.s.), 41.1, 41.4 (C-7, -9, a.s.), 42.8, 43.4 (C-2, -3, -5, -6, *A*), 58.0 (C-2, **A**), 64.3 (C-2, -3, a.s.), 64.7 (CH_2OH), 107.3 (C-5, a.s.), 164.3 (C-4, -6, T-1), 164.6 (C-2, T-0), 165.0 (C-4, T-0), 166.1 (C-6, T-0), 169.3 (C-2, T-1) ppm; *m*/*z* (ESI^+, MeOH in $CHCl_3$ 6:1) 952.6 (MNa^+) (0.4), 930.6 (MH^+) (3.5), 703.5 (0.6), 619.6 (3.2), 591.6 (1.0), 465.8 (2.4), 437.2 (2.1×10^5).

*5.1.6.2. 2-Chloro-4,6-bis{4-{6-{[1-hydroxy-2-(hydroxymethyl)but-2-yl]amino}-4-(1,4-dioxa-8-azaspiro[4.5]decan-8-yl)-s-triazin-2-yl}-piperazin-1-yl}-s-triazine (**8b**).* Yield 78%; white crystalline solid, mp 236–237 °C (crystallisation from EtOH/Et_2O). Found: C, 51.55; H, 6.89; N, 25.05%. $C_{41}H_{64}ClN_{17}O_8$ (957.48) requires C, 51.38; H, 6.73; N, 24.84%; R_f (66% toluene/*i*-PrOH) 0.70; ν_{max} (KBr) 3400, 2958, 2879, 1566, 1532, 1294, 1439, 1354, 1257, 1228, 1089, 1000, 977, 808, 731, 662 cm^{-1}; δ_H (400 MHz, DMSO-d_6, 353 K) 0.81 (6H, t,

J 7.2 Hz, CH_2CH_3), 1.62 (8H, t, *J* 4.8 Hz, H-6, -10, a.s.), 1.83 (4H, q, *J* 7.3 Hz, CH_2CH_3), 3.59 (4H, d, *J* 10.8 Hz, CH_2OH), 3.65 (4H, d, *J* 10.8 Hz, CH_2OH), 3.76 (16H, s: 8H, H-7, -9, a.s.; 8H, H-3, -5, *A*), 3.77 (8H, s, H-2, -6, *A*), 3.93 (8H, s, H-2, -3, a.s.), 4.94 (4H, br s, OH), 5.63 (2H, br s, NH) ppm; δ_C (100 MHz, DEPT, DMSO-d_6, 298 K) 8.2 (CH_2CH_3), 23.5 (CH_2CH_3), 34.9 (C-6, -10, a.s.), 41.2, 41.6 (C-7, -9, a.s.), 42.9 (C-3, -5, *A*), 43.4 (C-2, -6, *A*), 60.5 (C-2, **B**), 62.5 (C-2, -3, a.s.), 64.3 (CH_2OH), 107.2 (C-5, a.s.), 164.3 (C-4, -6, T-1), 164.6 (C-2, T-0), 164.9 (C-4, T-0), 165.8 (C-6, T-0), 169.3 (C-2, T-1) ppm; *m*/*z* (ESI^+, MeOH) 980.3 (MNa^+) (0.05), 958.3 (MH^+) (0.90), 619.4 (0.50), 479.7 (0.70), 424.2 (0.25), 371.6 (0.45), 320.5 (0.25), 263.5 (0.50×10^6).

*5.1.6.3. 2-Chloro-4,6-bis{4-{6-{[1,3-dihydroxy-2-(hydroxymethyl) prop-2-yl]amino}-4-(1,4-dioxa-8-azaspiro[4.5]decan-8-yl)-s-triazin-2-yl}-piperazin-1-yl}-s-triazine (**8c**).* Yield 86%; white crystalline solid, mp 248.2–249.4 °C (crystallisation from THF). Found: C, 48.84; H, 6.09; N, 25.01%. $C_{39}H_{60}ClN_{17}O_{10}$ (961.44) requires C, 48.67; H, 6.28; N, 24.74%; R_f (66% toluene/*i*-PrOH) 0.40; ν_{max} (KBr) 3387, 2934, 2879, 1564, 1492, 1439, 1364, 1286, 1257, 1229, 1113, 1085, 999, 977, 806, 661 cm^{-1}; δ_H (400 MHz, DMSO-d_6, 353 K) 1.63 (8H, br t, H-6, -10, a.s.), 3.72 (28H, s: 12H, CH_2OH; 16H, *A*), 3.76 (8H, t, *J* 5.6 Hz, H-7, -9, a.s.), 3.93 (8H, s, H-2, -3, a.s.), 4.10 (6H, br s, OH), 5.69 (2H, br s, NH) ppm; δ_C (100 MHz, DEPT, DMSO-d_6, 298 K) 34.9 (C-6, -10, a.s.), 41.2, 41.7 (C-7, -9, a.s.), 43.0 (C-3, -5, *A*), 43.4 (C-2, -6, *A*), 61.2 (C-2, -3, a.s.), 61.7 (C-2, **C**), 64.3 (CH_2OH), 107.2 (C-5, a.s.), 164.4 (C-4, -6, T-1), 164.8 (C-2, -4, T-0), 165.7 (C-6, T-0), 169.3 (C-2, T-1) ppm; *m*/*z* (ESI^+, ACN/H_2O): HRMS calcd for $C_{39}H_{61}N_{17}O_{10}$ (MH^+) 962.4476; found 962.4496 (100%).

*5.1.6.4. 2-Chloro-4,6-bis{4-{6-{[1-hydroxy-2-(methyl)prop-2-yl] amino}-4-(1,4-dioxa-8-azaspiro[4.5]decan-8-yl)-s-triazin-2-yl}-piperazin-1-yl}-s-triazine (**8d**).* Yield 68%; white crystalline solid, mp 244.8–246.1 °C (column chromatography, AcOEt/Ligroin 16:1). Found: C, 51.94; H, 6.45; N, 26.55%. $C_{39}H_{60}ClN_{17}O_6$ (897.46) requires C, 52.14; H, 6.73; N, 26.50%; R_f (94% AcOEt/Ligroin) 0.67; ν_{max} (KBr) 3350, 2958, 1544, 1489, 1438, 1362, 1256, 1226, 1090, 1002, 978, 941, 808, 661 cm^{-1}; δ_H (500 MHz, DMSO-d_6, 363 K) 1.33 (12H, s, Me), 1.62 (8H, t, *J* 5.8 Hz, H-6, -10, a.s.), 3.48 (4H, s, CH_2OH), 3.77 (8H, t, *J* 5.0 Hz, H-7, -9, a.s.; 16H, s, *A*), 3.93 (8H, s, H-2, -3, a.s.), 4.65 (2H, br s, OH), 5.66 (2H, br s, NH) ppm; δ_C (125 MHz, DEPT, DMSO-d_6, 298 K) 24.3 (Me), 34.9 (C-6, -10, a.s.), 41.0, 41.4 (C-7, -9, a.s.), 42.8 (C-3, -5, *A*), 43.4 (C-2, -6, *A*), 54.3 (C-2, **D**), 64.3 (C-2, -3, a.s.), 68.7 (CH_2OH), 107.3 (C-5, a.s.), 164.3 (C-4, -6, T-1), 164.6 (C-2, T-0), 165.0 (C-4, T-0), 166.0 (C-6, T-0), 169.3 (C-2, T-1) ppm; *m*/*z* (ESI^+, ACN in DCM) 936.5 (MK^+) (1.0), 920.5 (MNa^+) (0.5), 898.5 (MH^+) (5.3×10^6).

*5.1.6.5. 2-Chloro-4,6-bis{4-{4,6-bis{[1-hydroxy-2-(methyl)prop-2-yl]amino}-s-triazin-2-yl}piperazin-1-yl}-s-triazine (**8e**).* Yield 90%; white crystalline solid, mp 220–222 °C (crystallisation from EtOH/Et_2O). Found: C, 50.35; H, 6.88; N, 30.31%. $C_{33}H_{56}ClN_{17}O_4$ (789.44) requires C, 50.15; H, 7.14; N, 30.13%; R_f (66% toluene/*i*-PrOH) 0.75; ν_{max} (KBr) 3398, 2967, 2924, 2865, 1566, 1494, 1440, 1361, 1274, 1229, 1169, 1057, 998, 977, 811, 740, 502 cm^{-1}. δ_H (500 MHz, DMSO-d_6, 353 K) 1.34 (24H, s, Me), 3.47 (8H, s, CH_2OH), 3.71–3.83 (16H, m, *A*), 4.77 (4H, br s, OH), 5.58 (4H, s, NH) ppm; δ_C (125 MHz, DEPT, DMSO-d_6, 303 K) 24.4 (Me), 42.8 (C-3, -5, *A*), 43.1, 43.4 (C-2, -6, *A*), 54.2 (C-2, **D**), 69.0 (CH_2OH), 164.4 (C-4, -6, T-1), 164.5 (C-2, T-0), 165.7 (C-4, -6, T-0), 169.3 (C-2, T-1) ppm; *m*/*z* (ESI^+, acetone/DMSO diluted with ACN) 790 (MH^+) (3.6), 639.5 (0.5), 595.4 (0.6), 551.4 (0.5), 507.4 (0.4), 463.3 (0.2), 413.3 (0.2×10^5).

*5.1.7. Typical procedure for the synthesis of compounds **9a**–**e**. Preparation of compound **9a** (Scheme 3).* To anhyd K_2CO_3 (0.198 g, 1.438 mmol) suspended a dry THF (125 mL) boiling solution containing anhyd piperazine (0.495 g, 5.75 mmol), compound **8a** (1.336 g, 1.438 mmol) was added, with vigorous stirring, as five equal portions every 90 min. After each of these periods, TLC monitoring indicated complete consumption of **8a** (toluene/*i*-PrOH 2:1) and formation of **9a** (*i*-PrOH/aq NH_3 25%). The reaction mixture was filtered hot and solids were well washed with hot anhyd THF. The organic filtrate was evaporated under reduced pressure to dryness and the solid residue was separated by column chromatography on silica gel (*i*-PrOH/aq NH_3 25%) to yield pure product **9a** (1.100 g, 78% with respect to **8a**).

*5.1.7.1. 1-{4,6-Bis{4-{6-{[1,3-dihydroxy-2-(methyl)prop-2-yl] amino}-4-(1,4-dioxa-8-azaspiro[4.5]decan-8-yl)-s-triazin-2-yl}-piperazin-1-yl}-s-triazin-2-yl}-piperazine (**9a**).* Yield 78%; yellowish powder, mp 246–247 °C (column chromatography, *i*-PrOH/aq NH_3 25% 9:1). Found: C, 52.45; H, 6.90; N, 27.41%. $C_{43}H_{69}N_{19}O_8$ (979.56) requires C, 52.69; H, 7.10; N, 27.15%; R_f (90% *i*-PrOH/aq NH_3 25%) 0.50; ν_{max} (KBr) 3414, 2880, 1535m 1485, 1438, 1363, 1255, 1088, 1001, 945, 807, 738, 660 cm^{-1}; δ_H (400 MHz, DMSO-d_6, 353 K) 1.30 (6H, Me), 1.61 (8H, s, H-6, -10, a.s.), 2.77 (4H, br s, H-3, -5, *B*) 3.55 (4H, d, *J* 10.0 Hz, CH_2OH), 3.65 (4H, d, *J* 10.0 Hz, CH_2OH), 3.64–3.74 (28H, br m: 8H, H-7, -9, a.s.; 16H, *A*; 4H, H-2, -6, *B*), 3.80 (5H, br s: 4H, OH; 1H, *B*>NH), 3.93 (8H, s, H-2, -3, a.s.), 5.59 (2H, s, NH) ppm; δ_C (100 MHz, DEPT, DMSO-d_6, 298 K) 19.2 (Me), 34.9 (C-6, -10, a.s.), 41.1, 41.4 (C-7, -9, a.s.), 43.1, 43.2 (CH_2, *A*), 43.8 (C-2, -6, *B*), 45.6 (C-3, -5, *B*), 58.0 (C-2, **A**), 64.3 (C-2, -3, a.s.), 64.7 (CH_2OH), 107.3 (C-5, a.s.), 164.5 (C-2, T-0), 165.0 (C-4, T-0), 165.1 (C-2, T-1), 165.2 (C-4, -6, T-1), 166.1 (C-6, T-0) ppm; *m*/*z* (ESI^+ in MeOH diluted with $CHCl_3$/MeOH 6:1) 1002.7 (MNa^+) (0.2), 980.8 (MH^+) (6.0), 647.6 (3.6), 619.6 (4.2), 591.6 (1.4), 490.9 (2.2), 437.2 (1.4×10^5).

*5.1.7.2. 1-{4,6-Bis{4-{6-{[1-hydroxy-2-(hydroxymethyl)but-2-yl] amino}-4-(1,4-dioxa-8-azaspiro[4.5]decan-8-yl)-s-triazin-2-yl}-piperazin-1-yl}-s-triazin-2-yl}-piperazine (**9b**).* Yield 85%; yellowish powder, mp 243–244 °C (column chromatography, *i*-PrOH/aq NH_3 25% 9:1). Found: C, 53.83; H, 7.56; N, 26.65%. $C_{45}H_{73}N_{19}O_8$ (1007.59) requires C, 53.61; H, 7.30; N, 26.40%; R_f (90% *i*-PrOH/aq NH_3 25%) 0.48; ν_{max} (KBr) 3400, 2963, 1530, 1485, 1434, 1364, 1285, 1254, 1115, 1088, 1000, 945, 807, 739, 661 cm^{-1}; δ_H (400 MHz, DMSO-d_6, 353 K) 0.80 (6H, t, *J* 7.4 Hz, CH_2CH_3), 1.61 (8H, t, *J* 5.6 Hz, H-6, -10, a.s.), 1.84 (4H, q, *J* 7.3 Hz, CH_2CH_3), 2.82 (4H, t, *J* 5.0 Hz, H-3, -5, *B*), 3.58 (4H, d, *J* 10.8 Hz, CH_2OH), 3.64 (4H, d, *J* 10.4 Hz, CH_2OH), 3.69–3.76 (29H, m: 8H, H-7, -9, a.s.; 16H, *A*; 4H, H-2, -6, *B*; 1H, *B*>NH), 3.93 (8H, s, H-2, -3, a.s.), 4.58 (4H, br s, OH), 5.49 (2H, s, NH) ppm; δ_C (100 MHz, DEPT, DMSO-d_6, 298 K) 8.3 (CH_2CH_3), 23.5 (CH_2CH_3), 34.9 (C-6, -10, a.s.), 41.0, 41.6 (C-7, -9, a.s.), 43.0 (CH_2, *A*), 43.4 (C-2, -6, *B*), 45.3 (C-3, -5, *B*), 60.4 (C-2, **B**), 62.6 (C-2, -3, a.s.), 64.3 (CH_2OH), 107.3 (C-5, a.s.), 164.5, 164.6 (C-2, T-0), 165.06 (C-4, T-0), 165.15 (C-2, T-1), 165.24 (C-4, -6, T-1), 166.0 (C-6, T-0) ppm; *m*/*z* (ESI^+ in MeOH) 1030.4 (MNa^+) (0.02), 1008.4 (MH^+) (1.2), 504.7 (2.4), 447.7 (0.6), 413.2 (1.4), 339.6 (0.5), 288.6 (1.4×10^6).

*5.1.7.3. 1-{4,6-Bis{4-{6-{[1,3-dihydroxy-2-(hydroxymethyl)prop-2-yl]amino}-4-(1,4-dioxa-8-azaspiro[4.5]decan-8-yl)-s-triazin-2-yl}-piperazin-1-yl}-s-triazin-2-yl}-piperazine (**9c**).* Yield 73%; yellowish powder, mp 256–257.4 °C (column chromatography, *i*-PrOH/aq NH_3 25% 4:1). Found: C, 50.89; H, 7.03; N, 26.25%. $C_{43}H_{69}N_{19}O_{10}$ (1011.55) requires C, 51.03; H, 6.87; N, 26.29%; R_f (80% *i*-PrOH/aq NH_3 25%) 0.42; ν_{max} (KBr) 3408, 2931, 2880, 1531, 1480, 1436, 1364, 1284, 1254, 1111, 1085, 1000, 944, 806, 740, 661 cm^{-1}; δ_H (500 MHz, DMSO-d_6, 363 K) 1.62 (8H, t, *J* 5.8 Hz, H-6, -10, a.s.), 2.87 (4H, t, *J* 5.0 Hz, H-3, -5, *B*), 3.72 (12H, s, CH_2OH), 3.69–3.76 (29H, m: 8H, H-7, -9, a.s.; 16H, *A*; 4H, H-2, -6, *B*; 1H, *B*>NH), 3.93 (8H, s, H-2, -3, a.s.), 4.54 (6H, br s, OH), 5.55 (2H, s, NH) ppm; δ_C (125 MHz, DEPT, DMSO-d_6, 298 K) 34.9 (C-6, -10, a.s.), 41.1, 41.6 (C-7, -9, a.s.), 42.9, 43.0 (CH_2, *A*), 43.2 (C-2, -6, *B*), 45.0 (C-3, -5, *B*), 61.3 (C-2, -3, a.s.), 61.6 (C-2, **C**), 64.3 (CH_2OH), 107.2 (C-5, a.s.), 164.5 (C-2, T-0), 164.9

(C-4, T-0), 165.1 (C-2, T-1), 165.2 (C-4, -6, T-1), 166.1 (C-6, T-0) ppm; *m*/*z* (ESI^+, ACN diluted with DCM/DMSO 3:1) 1012.6 (MH^+) (2.25×10^7).

*5.1.7.4. 1-{4,6-Bis{4-{6-{[1-hydroxy-2-(methyl)prop-2-yl]amino}-4-(1,4-dioxa-8-azaspiro[4.5]decan-8-yl)-s-triazin-2-yl}-piperazin-1-yl}-s-triazin-2-yl}-piperazine (**9d**).* Yield 80%; yellowish powder, mp 254.2–255 °C (column chromatography, *i*-PrOH/aq NH_3 25% 9:1). Found: C, 54.57; H, 7.29; N, 27.85%. $C_{43}H_{69}N_{19}O_6$ (947.57) requires C, 54.47; H, 7.34; N, 28.07%; R_f (90% *i*-PrOH/aq NH_3 25%) 0.53; ν_{max} (KBr) 3300, 2958, 2925, 1536, 1489, 1438, 1363, 1254, 1117, 997, 944, 810, 743 cm^{-1}; δ_H (500 MHz, DMSO-d_6, 363 K) 1.33 (12H, s, Me), 1.61 (8H, t, *J* 5.5 Hz, H-6, -10, a.s.), 2.98 (4H, t, *J* 5.0 Hz, H-3, -5, *B*), 3.48 (4H, s, CH_2OH), 3.71–3.77 (25H, m: 8H, H-7, -9, a.s.; 16H, *A*; 1H, *B*>NH), 3.84 (4H, t, *J* 5.0 Hz, H-2, -6, *B*), 3.93 (8H, s, H-2, -3, a.s.), 4.66 (2H, br s, OH), 5.62 (2H, s, NH) ppm; δ_C (125 MHz, DEPT, DMSO-d_6, 298 K) 24.3 (Me), 34.9 (C-6, -10, a.s.), 41.0, 41.1, 41.4, 41.6 (C-7, -9, a.s.), 43.1 (CH_2, *A*; C-2, -6, *B*), 44.1 (C-3, -5, *B*), 54.3 (C-2, **D**), 64.3 (C-2, -3, a.s.), 68.7 (CH_2OH), 107.3 (C-5, a.s.), 164.6 (C-2, T-0), 165.1 (C-4, T-0), 165.15 (C-2, T-1), 165.21 (C-4, -6, T-1), 166.0 (C-6, T-0) ppm; *m*/*z* (ESI^+, ACN in DCM) 986.6 (MK^+) (0.1), 970.6 (MNa^+) (0.1), 948.6 (MH^+) (3.5×10^7).

*5.1.7.5. 1-{4,6-Bis{4-{4,6-bis{[1-hydroxy-2-(methyl)prop-2-yl]amino}-s-triazin-2-yl}-piperazin-1-yl}-s-triazin-2-yl}-piperazine (**9e**).* Yield 70%; white powder, mp 225–230 °C (column chromatography, EtOH/aq NH_3 25% 9:1). Found: C, 53.11; H, 8.09; N, 31.59%. $C_{37}H_{65}N_{19}O_4$ (839.55) requires C, 52.90; H, 7.80; N, 31.68%; R_f (90% EtOH/aq NH_3 25%) 0.30; ν_{max} (KBr) 3385, 3330, 2968, 2924, 1543, 1484, 1438, 1359, 1271, 1198, 1054, 999, 809 cm^{-1}; δ_H (500 MHz, DMSO-d_6, 353 K) 1.34 (24H, s, Me), 2.85 (4H, t, *J* 5.0 Hz, H-3, -5, *B*), 3.46 (8H, s, CH_2OH), 3.69–3.71 (13H, m: 8H, H-2, -6, *A*; 4H, OH; 1H, *B*>NH), 3.74–3.77 (12H, m: 4H, t, *J* 5.0, H-2, -6, *B*; 8H, H-3, -5, *A*), 5.53 (4H, s, NH) ppm; δ_C (125 MHz, DEPT, DMSO-d_6, 303 K) 24.4 (Me), 42.98 (CH_2, *A*), 43.05 (C-2, -6, *B*), 45.0 (C-3, -5, *B*), 54.2 (C-2, **D**), 69.0 (CH_2OH), 164.6 (C-2, T-0), 165.2 (C-2, T-1), 165.3 (C-4, -6, T-1), 165.7 (C-4, -6, T-0) ppm; *m*/*z* (ESI^+ in MeOH) 862.4 (MNa^+) (0.8), 840.5 (MH^+) (4.8), 809.5 (0.2), 768.4 (0.4), 696.3 (0.5), 624.2 (0.5), 552.2 (0.6), 413.2 (0.3), 276.5 (1.0×10^6).

*5.1.8. Typical procedure for the synthesis of compounds **10a–e**. Preparation of compound **10b** (Scheme 3).* To anhyd K_2CO_3 (0.100 g, 0.725 mmol) suspended in dry and cooled (−10 °C) THF (35 mL) solution containing compound **9b** (0.700 g, 0.694 mmol), cyanuric chloride (0.061 g, 0.331 mmol) as THF (3 mL) solution was injected slowly, under vigorous stirring. The reaction mixture was allowed to reach room temperature overnight and then heated at reflux for 16 h. Since the TLC monitoring ($CHCl_3$/*i*-PrOH 7:1) still indicated the presence of the unreacted **9b**, THF was replaced by 1,4-dioxane (35 mL) and refluxing was continued for an additional 6 h (TLC monitoring). The reaction mixture was evaporated under reduced pressure to dryness and the solid residue taken, at room temperature, with cooled water (6 mL) under vigorous stirring, filtered and washed with cooled water to neutrality. After drying at 80 °C to constant mass, the crude product was twice crystallised from minimum amount of boiling isopropanol to yield pure **10b** (0.640 g, 91% yield with respect to cyanuric chloride).

*5.1.8.1. 2-Chloro-4,6-bis{4-{4,6-bis{4-{6-{[1,3-dihydroxy-2-(methyl)prop-2-yl]amino}-4-(1,4-dioxa-8-azaspiro[4.5]decan-8-yl)-s-triazin-2-yl}-piperazin-1-yl}-s-triazin-2-yl}-piperazin-1yl}-s-triazine (**10a**).* Yield 87% (crystallisation from *i*-PrOH), 73% (column chromatography, $CHCl_3$/EtOH 7:1) yellowish powder, mp 255–256 °C. Found: C, 51.49; H, 6.81; N, 27.54%. $C_{89}H_{136}N_{41}$ (2070.08) requires C, 51.60; H, 6.62; N, 27.72%; R_f (87.5% $CHCl_3$/EtOH) 0.60; ν_{max} (KBr) 3394, 2925, 2878, 1537, 1484, 1435, 1363, 1256, 1087, 998, 807, 740, 661 cm^{-1}; δ_H (400 MHz, DMSO-d_6, 353 K) 1.30 (12H, Me), 1.61 (16H, s, H-6, -10, a.s.), 3.56 (8H, d, *J* 10.0 Hz, CH_2OH), 3.66 (8H, d, *J* 10.4 Hz, CH_2OH), 3.72–3.79 (64H, br m: 32H, *A*; 16H, *B*; 16H, H-7, -9, a.s.), 3.93 (16H, s, H-2, -3, a.s.), 4.60 (8H, br s, OH), 5.60 (4H, s, NH) ppm; δ_C (100 MHz, DEPT and QC, DMSO-d_6, 298 K) 19.3 (4C, Me), 34.9 (8C, C-6, -10, a.s.), 41.1 (8C, C-7, -9, a.s.), 43.1 (20C: 16C, *A*; 4C, C-3, -5, *B*), 43.5 (4C, C-2, -6, *B*), 58.0 (4C, C-2, **A**), 64.3 (8C, C-2, -3, a.s.), 64.8 (8C, CH_2OH), 107.3 (4C, C-5, a.s.), 164.4 (2C, C-4, -6, T-2), 164.6 (4C, C-2, T-0), 165.0 (4C, C-4, T-0), 165.2 (6C, T-1), 166.1 (4C, C-6, T-0), 169.4 (1C, C-2, T-2) ppm; *m*/*z* (ESI^+ in MeOH) 2092.6 (MNa^+) (1.6), 2071.7 (MH^+) (2.5), 1215.6 (1.4), 1036.4 (0.6), 913.7 (0.4×10^4).

*5.1.8.2. 2-Chloro-4,6-bis{4-{4,6-bis{4-{6-{[1-hydroxy-2-(hydroxymethyl)but-2-yl]amino}-4-(1,4-dioxa-8-azaspiro[4.5]decan-8-yl)-s-triazin-2-yl}-piperazin-1-yl}-s-triazin-2-yl}-piperazin-1yl}-s-triazine (**10b**).* Yield 91% (crystallisation from *i*-PrOH), 78% (column chromatography, $CHCl_3$/EtOH 7:1) yellowish powder, mp 254–255 °C. Found: C, 52.65; H, 6.98; N, 27.11%. $C_{93}H_{144}ClN_{41}O_{16}$ (2126.14) requires C, 52.49; H, 6.82; N, 26.99%; R_f (87.5% $CHCl_3$/EtOH) 0.56; ν_{max} (KBr) 3410, 2959, 2924, 2879, 1535, 1485, 1435, 1363, 1287, 1257, 1089, 998, 807, 661 cm^{-1}; δ_H (500 MHz, DMSO-d_6, 353 K) 0.81 (12H, br s, CH_2CH_3), 1.61 (16H, br s, H-6, -10, a.s.), 1.83 (8H, br q, *J* 7.7 Hz, CH_2CH_3), 3.59 (8H, br d, *J* 9.5 Hz, CH_2OH), 3.65 (8H, br d, *J* 11.0 Hz, CH_2OH), 3.71 (16H, br s, H-7, -9, a.s.), 3.76 (32H, br s, *A*), 3.79 (16H, br s, *B*), 3.93 (16H, s, H-2, -3, a.s.), 4.59 (8H, br s, OH), 5.50 (4H, s, NH) ppm; δ_C (125 MHz, DEPT and QC, DMSO-d_6, 298 K) 8.22 (4C, CH_2CH_3), 23.5 (4C, CH_2CH_3) 34.9 (8C, C-6, -10, a.s.), 41.0, 41.6 (8C, C-7, -9, a.s.), 43.1 (20C: 16C, *A*; 4C, C-3, -5, *B*), 43.4 (4C, C-2, -6, *B*), 60.3 (4C, C-2, **B**), 62.6 (8C, C-2, -3, a.s.), 64.3 (8C, CH_2OH), 107.2 (4C, C-5, a.s.), 164.3 (2C, C-4, -6, T-2), 164.47, 164.50, 164.56, 164.59, 164.64, 164.68, 164.73 (4C, C-2, T-0), 165.0 (4C, C-4, T-0), 165.20, 165.24 (6C, T-1), 166.0 (4C, C-6, T-0), 169.3 (1C, C-2, T-2) ppm; *m*/*z* (ESI^+ in MeOH) 2127.7 (MH^+) (0.40), 1564.4 (0.4), 1542.4 (0.65), 619.4 (0.85×10^5).

*5.1.8.3. 2-Chloro-4,6-bis{4-{4,6-bis{4-{6-{[1,3-dihydroxy-2-(hydroxymethyl)prop-2-yl]amino}-4-(1,4-dioxa-8-azaspiro[4.5]decan-8-yl)-s-triazin-2-yl}-piperazin-1-yl}-s-triazin-2-yl}-piperazin-1-yl}-s-triazine (**10c**).* Yield 56%; yellowish powder, mp 264–265 °C (column chromatography, eluent $CHCl_3$/EtOH 3.5:1). Found: C, 49.81; H, 6.33; N, 27.05%. $C_{89}H_{136}ClN_{41}O_{20}$ (2134.06) requires C, 50.05; H, 6.42; N, 26.89%; R_f (77.7% $CHCl_3$/EtOH) 0.66; ν_{max} (KBr) 3391, 2925, 2878, 1536, 1483, 1435, 1363, 1257, 1111, 1085, 997, 807, 737 cm^{-1}; δ_H (500 MHz, DMSO-d_6, 363 K) 1.63 (16H, t, *J* 5.3 Hz, H-6, -10, a.s.), 3.73 (24H, d, *J* 5.0 Hz, CH_2OH), 3.76 (64H, t, *J* 5.8 Hz: 16H, H-7, -9, a.s.; 32H, *A*; 8H, H-3, -5, *B*), 3.80 (8H, s, H-2, -6, *B*), 3.93 (16H, s, H-2, -3, a.s.), 4.51 (12H, t, *J* 5.3 Hz, OH), 5.56 (4H, s, NH) ppm; δ_C (125 MHz, DEPT and QC as 5 mM in DMSO-d_6, 298 K) 34.9 (4C, C-6, -10, a.s.), 41.1, 41.6 (8C, C-7, -9, a.s.), 42.8, 43.0 (16C, *A*), 43.3, (4C, C-3, -5, *B*), 43.5 (4C, C-2, -6, *B*), 61.2, 61.3 (12C, CH_2OH), 61.5, 61.6 (8C, C-2, **C**), 64.3 (8C, C-2, -3, a.s.), 107.2 (4C, C-5, a.s.), 164.36 (2C, C-4, -6, T-2), 164.41, 164.43, 164.47, 164.54 (4C, C-2, T-0), 164.9 (4C, C-4, T-0), 165.2, 165.3 (6C, T-1), 166.1 (4C, C-6, T-0), 169.3 (1C, C-2, T-2) ppm; *m*/*z* (ESI^+, CAN diluted with DCM/DMSO) 2174.0 ($M+1+K^+$) (0.4), 2157.9 ($M+1+Na^+$) (0.4), 2135.9 (M+2) (2.9), 1351.8 (1.9), 1140.7 (1.8) 1043.7 (6.7×10^4).

*5.1.8.4. 2-Chloro-4,6-bis{4-{4,6-bis{4-{6-{[1-hydroxy-2-(methyl)prop-2-yl]amino}-4-(1,4-dioxa-8-azaspiro[4.5]decan-8-yl)-s-triazin-2-yl}-piperazin-1-yl}-s-triazin-2-yl}-piperazin-1-yl}-s-triazine (**10d**).* Yield 98%; yellowish powder, mp 265–275 °C (dec); (crystallisation from EtOH). Found: C, 52.98; H, 7.01; N, 28.55%. $C_{89}H_{136}ClN_{41}O_{12}$ (2006.1) requires C, 53.24; H, 6.83; N, 28.60%; R_f (91% $CHCl_3$/*i*-PrOH) 0.46; ν_{max} (KBr) 3400, 2964, 2925, 2870, 1533,

1490, 1436, 1364, 1255, 1088, 997, 807, 737 cm^{-1}; δ_H (500 MHz, DMSO-d_6, 363 K) 1.34 (24H, s, Me), 1.61 (16H, *J* 5.5 Hz, H-6, -10, a.s.), 3.48 (8H, d, *J* 5.5 Hz, C*H*$_2$OH), 3.72 (32H, t, *J* 5.0 Hz: 16H, H-7, -9, a.s.; 16H, *A*), 3.77 (24H, t, *J* 5.5 Hz: 16H, *A*; 8H, H-3, -5, *B*), 3.80 (8H, s, H-2, -6, *B*), 3.93 (16H, s, H-2, -3, a.s.), 4.68 (4H, t, *J* 5.5 Hz, OH), 5.64 (4H, s, NH) ppm; δ_C (125 MHz, DEPT and QC as 5 mM in DMSO-d_6, 298 K) 24.4 (8C, Me), 34.9 (8C, C-6, -10, a.s.), 41.0, 41.4 (8C, C-7, -9, a.s.), 43.1 (20C: 16C, *A*; 4C, C-3, -5, *B*), 43.5 (4C, C-2, -6, *B*), 54.3 (4C, C-2, **D**), 64.3 (8C, C-2, -3, a.s.), 68.7 (4C, CH_2OH), 107.3 (4C, C-5, a.s.), 164.4 (2C, C-4, -6, T-2), 164.6 (4C, C-2, T-0), 165.1 (4C, C-4, T-0), 165.2, 165.3 (6C, T-1), 166.0 (4C, C-6, T-0), 169.3 (1C, C-2, T-2) ppm; *m*/*z* (ESI$^+$, ACN diluted with DCM) 2046.0 (MK^+) (0.80), 2030.0 (MNa^+) (1.45), 2008.0 (MH^+) (1.55×10^5).

*5.1.8.5. 2-Chloro-4,6-bis{4-{4,6-bis{4-{4,6-bis{[1-hydroxy-2-(methyl)prop-2-yl]amino}-s-triazin-2-yl}-piperazin-1-yl}-s-triazin-2-yl}-piperazin-1yl}-s-triazine (**10e**).* Yield 70% (crystallisation from EtOH) white powder, mp 260–270 °C (dec), 63% (column chromatography, $CHCl_3$/EtOH 5:1). Found: C51.88; H: 6.91; N: 32.29%. $C_{77}H_{128}ClN_{41}O_8$ (1790.06) requires: C, 51.62; H, 7.20; Cl, 1.98; N, 32.05%; R_f (83% $CHCl_3$/EtOH) 0.75; ν_{max} (KBr) 3402, 2970, 2926, 2863, 1547, 1484, 1437, 1361, 1265, 1232, 1199, 1177, 1056, 998, 809 cm^{-1}. δ_H (500 MHz, DMSO-d_6, 353 K) 1.33 (48H, s, Me), 3.47 (16H, d *J* 4.0 Hz, C*H*$_2$OH), 3.71–3.72 (16H, m, piperazine *A*), 3.75–3.77 (24H, m: 16H, *A*; 8H, H-3, -5, *B*), 3.80 (8H, s, H-2, -6, *B*), 4.76 (8H, t, *J* 5.5 Hz, OH), 5.53 (8H, s, NH) ppm; δ_C (100 MHz, DEPT and QC, DMSO-d_6, 298 K) 24.4 (16C, Me), 43.1 (24C: 16C, *A*; 8C, *B*), 54.2 (8C, C-2, **D**), 69.0 (8C, CH_2OH), 164.3 (2C, C-4, -6, T-2), 164.5 (4C, C-2, T-0), 165.2 (4C, C-4, -6, T-1), 165.7 (8C, C-4, -6, T-0), 165.9 (2C, C-2, T-1), 169.3 (1C, C-2, T-2); *m*/*z* (ESI$^+$, acetone-DMSO diluted with ACN) 1829.2 (MK^+) (0.5), 1814.2 (MNa^+) (1.1), 1791.3 (MH^+) (2.1×10^4).

*5.1.9. Typical procedure for the synthesis of compounds **11a**, **11b**, **11d** and **11e**. Preparation of compound **11b** (Scheme 3).* G-2 dendron **10b** (dried under high vacuum to constant mass then analytically weighted 0.515 g, 0.242 mmol), freshly prepared 4,4′-bipiperidine (dried under high vacuum to constant mass then analytically weighted 0.0193 g, 0.115 mmol), potassium carbonate (analytically weighted 0.035 g, 0.254 mmol) and freshly distilled dimethylformamide (DMF) (25 mL) were mixed together and the resulting suspension was heated at 100 °C (CARE! Avoid refluxing DMF to prevent solvent decomposition!) for 36 h (TLC monitoring, $CHCl_3$/EtOH 3:1 v/v). DMF was distilled under reduced pressure and the solid residue was taken with distilled water (10 mL), stirred at room temperature for 30 min then filtered off. The crude product was well washed with distilled water (×5 mL) to neutrality then dried at 70 °C to constant weight. The crude product was dissolved in distilled DMF (2 mL), then crystallised by adding anhyd diethyl ether (6 mL). The resulted suspension was cooled at −20 °C for 24 h, filtered off and well washed with anhyd diethyl ether to afford, after drying at 70 °C to constant weight, 0.345 g compound **11b** (69% yield with respect to 4,4′bipiperidine). Alternative isolation by column chromatography: the crude and dried product was first eluted on silica gel with $CHCl_3$/EtOH/Et_2O 3:1:1 to recover 0.041 g (0.019 mmol, 8%) unreacted chlorodendron **10b**. With the use of $CHCl_3$/EtOH 3:1 as eluent, 0.336 g (0.077 mmol) compound **11b** was isolated (68% yield with respect to 4,4′-bipiperidine).

*5.1.9.1. 1,1′-{4,6-Bis{4-{4,6-bis{4-{6-{[1,3-dihydroxy-2-(methyl)prop-2-yl]amino}-4-(1,4-dioxa-8-azaspiro[4.5]decan-8-yl)-s-triazin-2-yl}-piperazin-1-yl}-s-triazin-2-yl}-piperazin-1yl}-s-triazine-2-yl}-4,4′-bipiperidine (**11a**).* Yield 46% (column chromatography: $CHCl_3$/EtOH/Et_2O 3:1:0.7 to elute precursor **10a** then $CHCl_3$/EtOH 3:1 to elute **11a**) white powder, mp 261–262 °C. Found: C, 53.45; H, 7.09; N, 27.69%. $C_{188}H_{290}N_{84}O_{32}$ (4236.36) requires C, 53.27; H, 6.90; N, 27.76%; R_f (75% $CHCl_3$/EtOH) 0.75; ν_{max} (KBr) 3250, 2920, 2852, 1652, 1608, 1536, 1483, 1437, 1362, 1255, 1114, 997, 805, 779 cm^{-1}; δ_H (500 MHz, DMSO-d_6, 353 K) 1.30 (24H, s, Me), 1.61 (32H, t, *J* 5.5 Hz, H-6, -10, a.s.), 1.51–1.54, 1.70–1.72 (10H, m, H-3, -3′ -4, -4′ -5, -5′, bip.), 3.56 (16H, d, *J* 9.0 Hz, C*H*$_2$OH), 3.65 (16H, d, *J* 9.5 Hz, C*H*$_2$OH), 3.72–3.77 (136H, m: 64H, *A*; 32H, *B*; 32H, H-7, -9, a.s.; 8H, H-2, -2′, -6, -6′, bip.), 3.93 (32H, s, H-2, -3, a.s.), 4.58 (16H, br s, OH), 5.59 (8H, s, NH) ppm; δ_C (100 MHz, DEPT and QC as 5 mM in DMSO-d_6, 298 K) 19.2 (8C, Me), 34.9 (20C: 16C, C-6, -10, a.s.; 4C, C-3, -3′, -5, -5′, bip.), 41.1, 41.4 (22C: 16C, C-7, -9, a.s.; 6C, C-1, -1′, C-2, -2′, -6, -6′, bip.), 43.1 (48C: 32C, *A*; 16C, *B*), 58.0 (8C, C-2, **A**), 64.3 (16C, C-2, -3, a.s.), 64.7 (16C, CH_2OH), 107.2 (8C, C-5, a.s.), 164.5 (8C, C-2, T-0), 165.0 (10C: 8C, C-4, T-0; 2C, T-2); 165.2 (14C: 12C, C-2, -4, -6, T-1; 2C, T-2), 166.1 (10C: 8C, C-6, T-0; 2C, T-2); *m*/*z* (linear MALDI+, matrix 2,6-dihydroxybenzoic acid) 4237.132 (MH^+) (4200 a.u.).

*5.1.9.2. 1,1′-{4,6-Bis{4-{4,6-bis{4-{6-{[1-hydroxy-2-(hydroxymethyl)but-2-yl]amino}-4-(1,4-dioxa-8-azaspiro[4.5]decan-8-yl)-s-triazin-2-yl}-piperazin-1-yl}-s-triazin-2-yl}-piperazin-1yl}-s-triazine-2-yl}-4,4′-bipiperidine (**11b**).* Yield 69% (trituration from DMF/Et_2O 1:3), 68% (column chromatography: $CHCl_3$/EtOH/Et_2O 3:1:1 to elute precursor **10b** then $CHCl_3$/EtOH 3:1 to elute **11b**) white powder, mp 260–261 °C. Found: C, 53.97; H, 6.89; N, 27.19%. $C_{196}H_{306}N_{84}O_{32}$ (4348.49) requires C, 54.10; H, 7.09; N, 27.04%; R_f (75% $CHCl_3$/EtOH) 0.75; ν_{max} (KBr) 3402, 2931, 2878, 1671, 1534, 1483, 1435, 1364, 1254, 1089, 999, 806, 661 cm^{-1}; δ_H (500 MHz, DMSO-d_6, 353 K) 0.80 (24H, t, *J* 7.5 Hz, CH_2CH_3), 1.61 (42H, br s: 32H, H-6, -10, a.s.; 10H, H-3, -3′ -4, -4′, -5, -5′, bip.), 1.83 (16H, q, *J* 7.2 Hz, C*H*$_2$CH$_3$), 3.58 (16H, d, *J* 10.5 Hz, C*H*$_2$OH), 3.64 (16H, d, *J* 9.5 Hz, C*H*$_2$OH), 3.70–3.75 (136H, m: 64H, *A*; 32H, *B*; 32H, H-7, -9, a.s.; 8H, H-2, -2′, -6, -6′, bip.), 3.92 (32H, s, H-2, -3, a.s.), 4.59 (16H, br s, OH), 5.50 (8H, s, NH) ppm; δ_C (100 MHz, DEPT and QC as 5 mM in DMSO-d_6, 298 K) 8.3 (8C, CH_2CH_3), 23.5 (8C, CH_2CH_3), 35.0 (20C: 16C, C-6, -10, a.s.; 4C, C-3, -3′, -5, -5′, bip.), 41.6 (22C: 16C, C-7, -9, a.s.; 6C, C-1, -1′, C-2, -2′, -6, -6′, bip.), 43.1 (48C: 32C, *A*; 16C, *B*), 60.4 (8C, C-2, **B**), 62.5 (16C, C-2, -3, a.s.), 64.3 (16C, CH_2OH), 107.3 (8C, C-5, a.s.), 164.5, 164.7 (8C, C-2, T-0), 165.1 (10C: 8C, C-4, T-0; 2C, T-2); 165.3 (14C: 12C, C-2, -4, -6, T-1; 2C, T-2), 166.0 (10C: 8C, C-6, T-0; 2C, T-2); *m*/*z* (linear MALDI+, matrix 2,6-dihydroxybenzoic acid) 4348.4 (M^+) (100), 4247.0 (17), 3764.4 (27), 3098.9 (12), 1800.7 (18%).

*5.1.9.3. 1,1′-{4,6-Bis{4-{4,6-bis{4-{6-{[1-hydroxy-2-(methyl)prop-2-yl]amino}-4-(1,4-dioxa-8-azaspiro[4.5]decan-8-yl)-s-triazin-2-yl}-piperazin-1-yl}-s-triazin-2-yl}-piperazin-1yl}-s-triazine-2-yl}-4,4′-bipiperidine (**11d**).* Yield 48% (column chromatography: $CHCl_3$/EtOH/Et_2O 3:0.5:1.5 to elute precursor **10d** then $CHCl_3$/EtOH 3:0.5 to elute **11d**); grey powder, mp 272–282 °C (dec). Found: C, 55.15; H, 6.95; N, 28.81%. $C_{188}H_{290}N_{84}O_{24}$ (4108.41) requires C, 54.93; H, 7.11; N, 28.62; R_f (86% $CHCl_3$/EtOH) 0.52; ν_{max} (KBr) 3300, 2925, 2864, 1536, 1483, 1436, 1363, 1254, 1176, 1086, 994, 947, 810, 754, 659 cm^{-1}; δ_H (500 MHz, DMSO-d_6, 353 K) 1.32 (48H, s, Me), 1.60 (42H, br s: 32H, H-6, -10 a.s.; 10H, H-3, -3′ -4, -4′ -5, -5′, bip.), 3.47 (16H, br s, C*H*$_2$OH), 3.71–3.75 (136H, bm: 64H, *A*; 32H, *B*; 32H, H-7, -9, a.s.; 8H, H-2, -2′, -6, -6′, bip.), 3.91 (32H, s, H-2, -3, a.s.), 4.70 (8H, br s, OH), 5.64 (8H, br s, NH); δ_C (150 MHz, DEPT, DMSO-d_6, 298 K) 24.4 (Me), 34.9 (C-6, -10, a.s.; C-3, -3′, -5, 5′, bip.), 41.0 (C-7, -9, a.s.; C-2, -2′, -6, -6′, bip.), 43.1 (CH_2, *A*, *B*), 54.3 (C-2, **D**), 64.3 (C-2, -3, a.s.), 68.7 (CH_2OH), 107.3 (C-5, a.s.), 164.6 (C-2, T-0), 165.0, 165.2, 166.0 (T-0, -1, -2); *m*/*z* (linear MALDI+, matrix 2,6-dihydroxybenzoic acid) 4109.579 (MH^+) (2100), 4022.492 (300), 2100.322 (200), 1989.276 (7800 a.u.).

*5.1.9.4. 1,1′-{4,6-Bis{4-{4,6-bis{4-{4,6-bis{4-{4,6-bis[1-hydroxy-2-(methyl)prop-2-yl-amino]-s-triazin-2-yl}-piperazin-1-yl}-s-triazin-2-yl}-piperazin-1-yl}-s-triazin2-yl}-4,4′-bipiperidine (**11e**).* Yield 62% (column chromatography, eluent $CHCl_3$/EtOH 3.5:1), white powder, mp 265–275 °C (dec). Found: C53.71; H: 7.31; N: 32.19%. $C_{164}H_{274}N_{84}O_{16}$ (3676.32) requires: C, 53.55; H, 7.51; N, 31.98%; R_f (83% $CHCl_3$/EtOH) 0.23; ν_{max} (KBr) 3400, 2964, 2931, 2858, 1545,

1480, 1436, 1357, 1260, 1176, 997, 807, 737 cm^{-1}; δ_H (500 MHz, DMSO-d_6, 363 K) 1.27–1.46 (106H, m: 96H, Me; 10H, H-3, -3′, -4, -4′, -5, -5′, bip.), 3.47 (32H, s, CH_2OH), 3.71–3.72 (40H, m: 32H, *B*; 8H, H-2, -2′, -6, -6′, bip.), 3.76 (64H, s, *A*), 4.70 (16H, br d, *J* 8.0 Hz, OH), 5.48 (16H, s, NH) ppm; δ_C (100 MHz, DEPT and QC as 5 mM in DMSO-d_6, 298 K) 24.4 (32C, Me), 43.1 (52C: 32C, *A*; 16C, *B*; 4C, C-2, -2′, -6, -6′, bip.), 54.2 (16C, C-2, **D**), 69.0 (16C, CH_2OH), 164.6 (12C: 8C, C-2, T-0; 4C, T-1), 165.2 (18C: 16C, C-4, -6, T-0; 2C, T-2), 165.6 (12C: 8C, C-4, -6, T-1; 4C, C-4, -6, T-2); *m*/*z* (linear MALDI+ matrix 2,5-dihydroxybenzoic acid) 3677.38 (MH^+) (0.05), 3595.304 (0.18), 2034.284 (0.20), 1951.283 (0.80), 1800.181 (4.5), 1728.1 (1.3×10^4).

5.2. AFM analysis

Solutions of compounds **11e** (in DMSO), **11b** (in DMSO) and **11d** (in $CHCl_3$/EtOH 3:1) were chosen to make dendrimer self assemblies on mica solid support.

5.2.1. Sample preparation. Self-assembled dendrimer films were prepared by adsorption of each dendrimer from its bulk organic solution at three different concentrations (about 0.01 mM, 0.1 mM or 1 mM) on mica substrate situated in vertical position in each dendrimer solution. Alternatively, mica surface was also placed in the dendrimer solution oriented horizontally facing down in order to prevent the deposition of dendrimer aggregates (or nano particles) through sedimentation. Mica plates were maintained for various adsorption times (from 30 s to 60 min) at room temperature, by using a known protocol.[28] Thus, the adsorbed amount of dendrimer was monitored through the variation of the adsorption duration and of the dendrimer concentration in organic solutions. Prior to each adsorption experiment, the mica substrate was diced into 1 cm×1 cm plates and freshly cleaved before dendrimer adsorption. After the adsorption time, each sample was withdrawn and gently rinsed with suitable solvent to take out the excess of dendrimers, weakly adsorbed on the self-assembled films. Then, the dendrimer films were dried at room temperature, under a beaker and prepared for AFM investigation. As an alternative, some samples were dried under a weak but stable nitrogen stream and then immediately subjected to AFM imaging. In the last situation, the drying took less than 0.5 min. As recently mentioned,[29] such a short drying process does not provoke the surface aggregation of biomolecules. Afterwards, all dried samples were used for AFM examination. The AFM images on samples prepared in both drying procedures show no observable drying patterns under the experimental working conditions. An analysis of AFM images shows that the dendrimer adsorption reaches a steady state saturation of mica surface in about 1 h at 20 °C for each used dendrimer at 1 mM bulk concentration. This finding indicates that 1 mM concentration can be considered an optimal bulk concentration to produce in about 1 h a rather compact adsorbed film of each dendrimer on mica. Consequently, the dendrimer films obtained through adsorption of 1 h from 1 mM dendrimer solution were apparently at the saturation of mica surface with dendrimers.

5.3. AFM measurements

All samples were investigated by AFM operating in tapping mode, to minimize the force exerted from the scanning tip of AFM cantilever on the adsorbed dendrimer layers. The AFM imaging was performed on a JEOL 4210 instrument. All measurements were performed in air at room temperature for high lateral image resolution. Standard cantilevers, non-contact conical shaped of silicon nitride coated with aluminium, were used. The sharpened tips were on cantilevers with a resonant frequency in the range of 200–300 kHz and with a spring constant of 17.5 N/m. AFM images were collected at a scan rate of about 1 Hz. Structural features of the dendrimer adsorbed films were visualised from large scan area of 20 μm×20 μm to relatively small areas of 1 μm×1 μm and 0.2 μm×0.2 μm. AFM observations were repeated on different areas of the same film. The images were obtained from at least five macroscopically separated areas on each sample. All images were processed using the standard procedures for AFM. AFM images (512×512 pixels) consist of multiple scans on *x* direction displaced laterally from each other in *y* direction. All AFM experiments were carried out under ambient laboratory conditions (about 20 °C) as previously reported.[28] The AFM images on samples prepared in both drying procedures show no observable drying patterns under the experimental working conditions. This study is done under comparable surface packing density, at the same adsorption time (1 h at room temperature), at the saturation of surface with dendritic molecules.

Acknowledgements

The financial support from Grant provided by the Research Council Romania (Project PN-II-ID-PCE-3-0128) is gratefully acknowledged. The financial support from Grant provided by the *Research Council Romania* (Project BD 1482) is gratefully acknowledged by F.P. O.M. thanks for '*Investing in people!*' Ph.D. scholarship, Project co-financed by the SECTORAL OPERATIONAL PROGRAM FOR HUMAN RESOURCES DEVELOPMENT 2007–2013 Priority Axis 1. 'Education and training in support for growth and development of a knowledge based society' Key area of intervention 1.5: Doctoral and post-doctoral programs in support of research. Contract no.: POSDRU/88/1.5/S/60185—'INNOVATIVE DOCTORAL STUDIES IN A KNOWLEDGE BASED SOCIETY' Babeş-Bolyai University, Cluj-Napoca, Romania'. The computational centre of the University of Reims Champagne-Ardenne (ROMEO, http://www.romeo2.fr) is acknowledged for the CPU time donated.

Supplementary data

SD 1. Calculation of the rotational barrier $\Delta G^{\neq}$ of compound **2a**; SD 2. Assignment of *anti* versus *syn* rotameric occurrence in the case of compound **4b** according to the 'dipole rule' (Fig. I); SD 3. Rotational dynamic behaviour of compound **4b** on 400 MHz ^{1}H NMR timescale (Fig. II); SD 4. Calculation of the rotational barrier $\Delta G^{\neq}$ of compounds **4a**–**d** (Table I); SD 5. Rotational dynamic behaviour of compound **4e** (Fig. III); SD **6**. NMR spectra of compound **6a** (Fig. IVa–c); SD 7. Table II, VT NMR behaviour of melamines **5a**, **5b**, **7a**, **7b**, **7e** about the bonds C(*s*-triazine)–N(exocyclic) in DMSO-d_6; SD 8. Mass spectra of compounds **11a**–**e** (Fig. VIa–e); SD 9. 2D DOSY ^{1}H NMR charts of compounds **10a**, **11b**, **10c**, **11c**, **10e**, **11e** (Fig. VIIa–f); SD 10. Comparative VT NMR behaviour of G-1 chlorodendron **8b** versus G-1 dendritic melamine **9b** (Fig. Va and b); SD 11. Table III: selected (VT) ^{1}H NMR data of compounds **8**–**11** for their behaviour about the peripheral NH and OH groups in DMSO-d_6; SD 12. Peripheral rotamerism in *Ethylserinol* **B** derivatives **4b**, **6b**, **8**–**10b** on ^{13}C NMR timescale (Fig. VIII); SD 13. Integration of C-*s*-triazines signals in G-2 chlorodendrons **10a**–**e** (Fig. IX); SD 14. Relevant NMR spectra of compounds **11a**, **11b**, **11d** and **11e** (Fig. Xa–d). Supplementary data associated with this article can be found in the online version, at http://dx.doi.org/10.1016/j.tet.2012.07.096.

References and notes

1. Reviews: (a) Darabantu, M. *Curr. Org. Synth.* **2010**, *7*, 235–275; (b) Darabantu, M. *Curr. Org. Synth.* **2010**, *7*, 120–152.
2. (a) Newkome, G. R.; Yao, Z.; Baker, G. R.; Gupta, V. K. *J. Org. Chem.* **1985**, *50*, 2003–2004; (b) Newkome, G. R.; Schreiner, C. *Chem. Rev.* **2010**, *110*, 6338–6442.
3. Vögtle, F.; Richard, G.; Werner, N. *Dendrimer Chemistry (Concepts, Syntheses, Properties, Applications)*; WILEY-VCH: Weinheim, 2009, pp 7–22, 25–44.

4. (a) Ballico, M.; Drioli, S.; Bonora, G. M. *Eur. J. Org. Chem.* **2005**, 2064–2073; (b) Gillies, E. R.; Fréchet, J. M. J. *Bioconjugate Chem.* **2005**, *16*, 361–368; (c) Wharton, T.; Wilson, L. J. *Tetrahedron Lett.* **2002**, *43*, 561–564; (d) Wharton, T.; Kini, V. U.; Mortis, R. S.; Wilson, L. J. *Tetrahedron Lett.* **2001**, *42*, 5159–5162; (e) Wharton, T.; Wilson, L. J. *Bioorg. Med. Chem.* **2002**, *10*, 3545–3554; (f) Sørbye, K.; Carlssen, P. H. J. *Synth. Commun.* **1997**, *27*, 2813–2816; (g) Wang, A. Y.; Li, J. J.; Chen, H.; Peng, X. *J. Am. Chem. Soc.* **2002**, *124*, 2293–2298; (h) Leopoittevin, B.; Matmour, R.; Francis, R.; Taton, D.; Gnanou, Y. *Macromolecules* **2005**, *38*, 3120–3128.
5. (a) Zhang, W.; Simanek, E. E. *Org. Lett.* **2000**, *2*, 843–845; (b) Zhang, W.; Simanek, E. E. *Tetrahedron Lett.* **2001**, *42*, 5355–5357; (c) Zhang, W.; Nowlan, D. T.; Thomson, L. M.; Lackowski, M. W.; Simanek, E. E. *J. Am. Chem. Soc.* **2001**, *123*, 8914–8922; (d) Steffensen, M. B.; Simanek, E. E. *Org. Lett.* **2003**, *5*, 2359–2361; (e) Steffensen, M. B.; Simanek, E. E. *Angew. Chem., Int. Ed.* **2004**, *43*, 5178–5180; (f) Moreno, X. K.; Simanek, E. E. *Tetrahedron Lett.* **2008**, *49*, 1152–1154; (g) Hollink, E.; Simanek, E. E. *Org. Lett.* **2006**, *8*, 2293–2295; (h) Chouai, A.; Simanek, E. E. *J. Org. Chem.* **2007**, *73*, 2357–2366; (i) Crampton, H.; Hollink, E.; Perez, L. ,M.; Simanek, E. E. *New J. Chem.* **2007**, *31*, 1283–1290; (j) Chouai, A.; Venditto, V. J.; Simanek, E. E. *Org. Synth.* **2009**, *86*, 151–160; (k) Chouai, A.; Venditto, V. J.; Simanek, E. E. *Org. Synth.* **2009**, *86*, 141–150; (l) Mintzer, M. A.; Perez, L. M.; Simanek, E. E. *Tetrahedron Lett.* **2010**, *51*, 1631–1634; (m) Lim, J.; Mintzer, M. A.; Perez, L. M.; Simanek, E. E. *Org. Lett.* **2010**, *12*, 1148–1151.
6. (a) Umali, A. P.; Simanek, E. E. *Org. Lett.* **2003**, *5*, 1245–1247; (b) Zhang, W.; Tichy, S. E.; Perez, L. M.; Maria, C. G.; Lindahl, P. A.; Simanek, E. E. *J. Am. Chem. Soc.* **2003**, *125*, 5086–5094; (c) Umali, A. P.; Crampton, L. H.; Simanek, E. E. *J. Org. Chem.* **2007**, *72*, 9866–9874.
7. (a) Zhang, W.; Gonzalez, S. O.; Simanek, E. E. *Macromolecules* **2002**, *35*, 9015–9021; (b) Acosta, E. J.; Deng, Y.; White, G. N.; Dixon, J. B.; McInnes, K. J.; Senseman, S. A.; Frantzen, A. S.; Simanek, E. E. *Chem. Mater.* **2003**, *15*, 2903–2909; (c) Acosta, E. J.; Gonzalez, S. O.; Simanek, E. E. *J. Polym. Sci., Part A* **2005**, *43*, 168–177; (d) Yoo, S.; Lunn, D. J.; Gonzalez, S.; Ristich, J. A.; Simanek, E. E.; Shantz, D. *Chem. Mater.* **2006**, *18*, 2935–2942; (e) Lai, L. L.; Wang, L. Y.; Lee, C. H.; Lin, C. Y.; Cheng, K. L. *Org. Lett.* **2006**, *8*, 1541–1544; (f) Lai, L. L.; Lee, C. H.; Wang, L. Y.; Cheng, K. L.; Hsu, H. F. *J. Org. Chem.* **2008**, *73*, 485–490; (g) Yooa, S.; Yeua, S.; Sherman, R. L.; Simanek, E. E.; Shantza, D. F.; Ford, D. M. *J. Membr. Sci.* **2009**, *334*, 16–22; (h) Lalwani, S.; Venditto, V. J.; Chouai, A.; Rivera, E. G.; Shaunak, S.; Simanek, E. E. *Macromolecules* **2009**, *42*, 3152–3161.
8. (a) Bell, S. A.; McLean, M. E.; Oh, S.-K.; Tichy, S. E.; Zhang, W.; Corn, R. M.; Crooks, R. M.; Simanek, E. E. *Bioconjugate Chem.* **2003**, *14*, 488–493; (b) Neerman, M. F.; Zhang, W.; Parrish, A. R.; Simanek, E. E. *Int. J. Pharm.* **2004**, *281*, 129–132; (c) Chen, H. T.; Neerman, M. F.; Parrish, A. R.; Simanek, E. E. *J. Am. Chem. Soc.* **2004**, *126*, 10044–10048; (d) Lim, J.; Simanek, E. E. *Mol. Pharmaceut.* **2005**, *2*, 273–277; (e) Venditto, V. J.; Allred, K.; Allred, C. D.; Simanek, E. E. *Chem. Commun.* **2009**, 5541–5542; (f) Merkel, M. O.; Mintzer, M. A.; Sitterberg, J.; Bakowsky, U.; Simanek, E. E.; Kissel, T. *Bioconjugate Chem.* **2009**, *20*, 1799–1806; (g) Lim, J.; Venditto, V. J.; Simanek, E. E. *Bioorg. Med. Chem.* **2010**, *18*, 5749–5753; (h) Astruc, D.; Boisselier, E.; Ornelas, C. *Chem. Rev.* **2010**, *110*, 1857–1959.
9. (a) Steffensen, M. B.; Hollink, E.; Kuschel, F.; Bauer, M.; Simanek, E. E. *J. Polym. Sci., Part A: Polym. Chem.* **2006**, *44*, 3411–3433; (b) Crampton, H. L.; Simanek, E. E. *Polym. Int.* **2007**, *56*, 489–496; (c) Simanek, E. E.; Abdou, H.; Lalwani, S.; Lim, J.; Mintzer, M.; Venditto, V. J.; Vittur, B. *Proc. Roy. Soc. A. Ser. A* **2010**, *466*, 1445–1468.
10. (a) Kraiz, B. O.; Remizov, A. L. *Zh. Org. Khim.* **1979**, *15*, 1282–1289; (b) Baxi, G.; Pandya, A.; Pakikh, A. R. *J. Inst. Chem. (India)* **1996**, *68*, 44–45.
11. (a) Darabantu, M.; Pintea, M.; Fazekas, M.; Lameiras, P.; Berghian, C.; Delhom, I.; Silaghi-Dumitrescu, I.; Plé, N.; Turck, A. *Lett. Org. Chem.* **2006**, *3*, 905–910; (b) Pintea, M.; Fazekas, M.; Lameiras, P.; Cadis, I.; Berghian, C.; Silaghi-Dumitrescu, I.; Popa, F.; Bele, C.; Plé, N.; Darabantu, M. *Tetrahedron* **2008**, *64*, 8851–8870.
12. For example, for the preparation of certain (un)symmetrically *N*-substituted melamines claimed as of pharmaceutical interest it was the ethylene ketal of piperidone the last amino-nucleophile to be used against the corresponding 2-chloro-4,6-diamino-s-triazines, i.e., the strategy one must deduce indirectly. See Henkin, J.; Davidson, D. J.; Sheppard, G.; Woods, S.; Keith, W.; McCroskey, R. W. (Abbott Laboratories, USA). PCT Int. Appl. WO 9931088, June 24, 1999 (e.g., U.S. Patent 6,150,362, 2000; U.S. Patent 6,288,228, 2001; E.P. 1037886) cf. *Chem. Abstr.* **1999**, *131*, 58855.
13. (a) Mc Elvain, S. M.; Mc Mahon, R. *J. Am. Chem. Soc.* **1949**, *71*, 901–906; (b) Popa, F.; Simioanca, I.; Pintea, M.; Fazekas, M.; Gratecap, L.; Berghian, C.; Batiu, C.; Darabantu, M. *Stud. U. Babes-Bol. Che.* **2008**, *LIII*, 5–13; (c) Popa, F.; Moldovan, O.; Iusco, M.; Lameiras, P.; Batiu, C.; Ramondenc, Y.; Darabantu, M. *Stud. U. Babes-Bol. Che.* **2009**, *LIV*, 237–248; (d) Popa, F.; Lameiras, P.; Henon, E.; Moldovan, O.; Martinez, A.; Batiu, C.; Ramondenc, Y.; Darabantu, M. *Can. J. Chem.* **2011**, *89*, 1–15; (e) Stach, K.; Thiel, M.; Bickelhaupt, F. *Monatsh. Chem.* **1962**, *93*, 1090–1106.
14. Moreno, X. K.; Simanek, E. E. *Macromolecules* **2008**, *41*, 4108–4114.
15. (a) To our knowledge, there is just one patent referring to amination of cyanuric chloride with the use of 2-amino-2-methylpropanol, the resulting chlorodiamino-*s*-triazine being claimed as rubber-to-metal adhesion promoter. See Seibert, R. F.; Wheeler, E. L.; Barrows, F. H.; True, W. R. (Uniroyal Chemical Co., Inc., USA). U.S. Patent 5,283,274; c.f. *Chem. Abstr.* **1995**, *122*, P11925; (b) Thurston, J. T.; Dudley, J. R.; Kaiser, D. W.; Hechenbleikner, I.; Schaefer, F. C.; Holm-Hansen, D. *J. Am. Chem. Soc.* **1951**, *73*, 2981–2983.
16. (a) Menicagli, R.; Malanga, C.; Peluso, P. *Synth. Commun.* **1994**, *24*, 2153–2158; (b) Samaritani, S.; Peluso, P.; Malanga, C.; Menicagli, R. *Eur. J. Org. Chem.* **2002**, *9*, 1551–1555; (c) Cuthberson, W. W.; Moffatt, J. S. *J. Chem. Soc.* **1948**, 561–564.
17. (a) de Gennes, P. G.; Hervet, H. *J. Phys. Lett. Fr. (Paris)* **1983**, *44*, L351–L361; (b) Tomalia, D. A.; Naylor, A.; Goddard, W. A., III. *Angew. Chem., Int. Ed. Engl.* **1990**, *29*, 138–175.
18. Smith, C. R. *J. Am. Chem. Soc.* **1928**, *50*, 1936–1938.
19. For example in the case of the well known herbicide ATRAZINE® (2-chloro-4-ethylamino-6-isopropylamino-*s*-triazine) see: (a) Drakenberg, T.; Forsen, S. *J. Chem. Soc., Chem. Commun.* **1971**, 1404–1405; (b) Mirvish, S. S.; Gannett, P.; Babcook, D. M.; Williamson, D.; Chen, S. C.; Weisenburger, D. D. *J. Agric. Food Chem.* **1991**, *39*, 1205–1210.
20. (a) Willner, I.; Rosengaus, J.; Eichen, Y. J. *Phys. Org. Chem.* **1993**, *6*, 29–43; (b) Katritzky, A. R.; Ghiviriga, I.; Oniciu, D. C.; Barkock, A. *J. Chem. Soc., Perkin Trans. 2* **1995**, 785–792; (c) Katritzky, A. R.; Ghiviriga, I.; Steel, P. G.; Oniciu, D. C. *J. Chem. Soc., Perkin Trans. 2* **1996**, 443–447; (d) Ghiviriga, I.; Oniciu, D. C. *Chem. Commun.* **2002**, 2718–2719; (e) Amm, M.; Platzer, N.; Guilhem, J.; Bouchet, J. P.; Volland, J. P. *Magn. Reson. Chem.* **1998**, *36*, 587–596; (f) Amm, M.; Platzer, N.; Bouchet, J. P.; Volland, J. P. *Magn. Reson. Chem.* **2001**, *39*, 77–84; (g) Birkett, H. E.; Harris, R. K.; Hodgkinson, P.; Carr, K.; Charlton, M. H.; Cherryman, J. C.; Chippendale, A. M.; Glover, R. P. *Magn. Reson. Chem.* **2000**, *38*, 504–511; (h) Birkett, H. E.; Cherryman, J. C.; Chippendale, A. M.; Evans, J. O. S.; Harris, R. K.; James, M.; King, I. J.; Mc Pherson, G. *Magn. Reson. Chem.* **2003**, *41*, 324–336.
21. (a) Fazekas, M.; Pintea, M.; Lameiras, P.; Lesur, A.; Berghian, C.; Silaghi-Dumitrescu, I.; Plé, N.; Darabantu, M. *Eur. J. Org. Chem.* **2008**, *14*, 2473–2494; (b) Moldovan, O.; Lameiras, P.; Henon, E.; Popa, F.; Martinez, A.; Harakat, D.; Sacalis, C.; Ramondenc, Y.; Darabantu, M. *Cent. Eur. J. Chem.* **2012**, *10*, 1119–1136.
22. (a) Eliel, E. L.; Wilen, H. S. *Stereochemistry of the Organic Compounds*; John Wiley & Sons: New York, NY, Chichester, UK, Brisbane, Toronto, Singapore, 1994, pp 465, 503–507, 1200, 1206; (b) Friebolin, H. *Basic One- and Two Dimensional NMR Spectroscopy*; VCH: Weinheim, New York, NY, 1991, pp 93, 263–291; (c) Gutowski, H. S.; Holm, C. H. *J. Chem. Phys.* **1956**, *25*, 1228–1234; (d) Shanan-Atidi, H.; Bar Eli, R. H. *J. Phys. Chem.* **1970**, *74*, 961–963; (e) For example, **6a**, $\Delta\delta_C$=0.3 ppm (C-α' vs -α") we have $\Delta\nu$=0.3×100=30 Hz. The rate constant of the first order kinetically exchange process occurring at 298 K was $k^1_{298} = 30\ s^{-1}$. The rotational time of life of azaspirane about the C(*s*-triazine)–N(azaspirane) bond at 298 K should be $\tau = 1/k^1_{298} > 0.033$ sfor the two broad lines be observed on 100 MHz time scale.
23. (a) Grosu, I.; Mager, S.; Ple, G.; Horn, M. *J. Chem. Soc., Chem. Commun.* **1995**, 167–168; (b) Darabantu, M.; Ple, G.; Silaghi-Dumitrescu, I.; Maiereanu, C.; Turos, G.; Silberg, I. A.; Mager, S. *Tetrahedron* **2000**, *56*, 3785–3798; (c) Cismas, C.; Terec, A.; Mager, S.; Grosu, I. *Curr. Org. Chem.* **2005**, *9*, 1287–1314.
24. (a) Darabantu, M.; Maiereanu, C.; Silaghi-Dumitrescu, I.; Toupet, L.; Condamine, E.; Ramondenc, I.; Berghian, G.; Ple, G.; Ple, N. *Eur. J. Org. Chem.* **2004**, *12*, 2644–2661; (b) Berghian, C.; Lameiras, P.; Toupet, L.; Condamine, E.; Ple, N.; Turck, A.; Maiereanu, C.; Darabantu, M. *Tetrahedron* **2006**, *62*, 7319–7338.
25. Kessler, H. *Angew. Chem., Int. Ed. Engl.* **1982**, *21*, 512–523 for $[\Delta\delta_{NH}/\Delta T]\times10^3$, we adopted negative values (Table 2, Chart 3) rather than positive, due to a reversed difference in the calculation of $\Delta\delta_{NH}$ (see also Ref. 14).
26. (a) Thureau, P.; Ancian, B.; Viel, S.; Thévand, A. *Chem. Commun.* **2006**, 200–202; (b) Thureau, P.; Ancian, B.; Viel, S.; Thévand, A. *Chem. Commun.* **2006**, 1884–1886; (c) Stejskal, O. E.; Tanner, J. E. *J. Chem. Phys.* **1965**, *42*, 288–292; (d) Stilbs, P. *Prog. Nucl. Magn. Reson. Spectrosc.* **1987**, *17*, 1–45; (e) Karger, J.; Pfeifer, H.; Heink, W. *Adv. Magn. Reson.* **1988**, *12*, 1–88.
27. (a) Bakshi, M. S.; Sood, R.; Kaur, G.; Sakai, K.; Yoshimura, T.; Esumi, K. *Colloid Polym. Sci.* **2005**, *284*, 74–79; (b) Cahill, B. B.; Papastavrou, G.; Koper, G. J. M. M.; Borkovec, M. *Langmuir* **2008**, *24*, 465–473; (c) Majoros, I. J.; Williams, C. R.; Tomalia, D. A.; Baker, J. R., Jr. *Macromolecules* **2008**, *41*, 8372–8379; (d) Palui, G.; Garai, A.; Nanda, J.; Nandi, A. K.; Banerjee, A. *J. Phys. Chem. B* **2010**, *114*, 1249–1256.
28. (a) Tomoaia-Cotisel, M. The Nanostructure Formation of the Globular Seed Storage Protein on Different Solid Surfaces Studied by Atomic Force Microscopy In *Convergence of Micro-Nano-Biotechnologies*; Zaharescu, M., Burzo, E., Dumitru, L., Kleps, I., Dascalu, D., Eds.; Series in Micro and Nanoengineering; Romanian Academy: Bucharest, 2006; Vol. 9, pp 147–161; (b) Horovitz, O.; Tomoaia, G.; Mocanu, A.; Yupsanis, T.; Tomoaia-Cotisel, M. *Gold Bull.* **2007**, *40*, 295–304; (c) Mocanu, A.; Cernica, I.; Tomoaia, G.; Bobos, L. D.; Horovitz, O.; Tomoaia-Cotisel, M. *Colloids Surf., A: Physicochem. Eng. Aspects* **2009**, *338*, 93–101; (d) Zdrenghea, U. V.; Tomoaia, G.; Pop-Toader, D. V.; Mocanu, A.; Horovitz, O.; Tomoaia-Cotisel, M. *Comb. Chem. High Throughput Screen.* **2011**, *14*, 237–247.
29. Wang, X.; Wang, Y.; Xu, H.; Shan, H.; Lu, J. R. *J. Colloid Interface Sci.* **2008**, *323*, 18–25.